This article has been accepted for inclusion in a future issue of this journal. Content is final as presented, with the exception of pagination.

Small Fault Detection of Discrete-Time Nonlinear Uncertain Systems

Jingting Zhang, Chengzhi Yuan, *Member, IEEE*, Paolo Stegagno, *Member, IEEE*, Haibo He, *Fellow, IEEE*, and Cong Wang, *Member, IEEE*

***Abstract*—This article investigates the problem of small fault detection (sFD) for discrete-time nonlinear systems with uncertain dynamics. The faults are considered to be "small" in the sense that the system trajectories in the faulty mode always remain close to those in the normal mode, and the magnitude of fault can be smaller than that of the system's uncertain dynamics. A novel adaptive dynamics learning-based sFD framework is proposed. Specifically, an adaptive dynamics learning approach using radial basis function neural networks (RBF NNs) is first developed to achieve locally accurate identification of the system uncertain dynamics, where the obtained knowledge can be stored and represented in terms of constant RBF NNs. Based on this, a novel residual system is designed by incorporating a newmechanism of absolute measurement of system dynamics changes induced by small faults. An adaptive threshold is then developed for real-time sFD decision making. Rigorous analysis is performed to derive the detectability condition and the analytical upper bound for sFD time. Simulation studies, including an application to a three-tank benchmark engineering system, are conducted to demonstrate the effectiveness and advantages of the proposed approach.**

***Index Terms*—Adaptive dynamics learning, discrete-time nonlinear uncertain systems, neural networks (NNs), small fault detection (sFD).**

I. Introduction

FAULT detection (FD) is an important issue in modern engineering systems and has received a great deal of attention to date (see [1]–[4], [40], [41]). Its primary objective is to identify the occurrence of system faults during real-time operation. Prompt and accurate FD is crucial for reliable and effective operations of many engineering systems especially those of critical safety, such as aero-engines, chemical processes, power networks, etc.

The past decades have witnessed tremendous progress in FD research, leading to a large variety of FD methods, which in general can be categorized as the model-based methods [1], signal-based methods [2], knowledge-based methods [5], and their hybridizations [3]. A comprehensive review of the FD literature has been nicely summarized in [6] and [7]. In particular, compared with the other methods, the model-based method has its unique advantage in providing a deeper insight into the dynamical behaviors of the system, facilitating more efficient and accurate FD under the dynamical process [6]. This has motivated considerable research efforts in recent years dedicated to the development of model-based FD methods. For example, Koenig [8] proposed a so-called proportional multiple–integral observer for linear descriptor systems with faults and unknown disturbed inputs. In [9], the FD problem was solved for nonlinear switched stochastic systems using filtering techniques. Li *et al.* [39] developed a polynomial fuzzy FD filter to investigate the FD problem for nonlinear discrete-time networked systems. A total measurable fault information residual method was proposed and refined in [10] and [11] for FD of LTI closed-loop systems. More recently, the model-based FD methods have been further extended to more challenging problems, such as fault-tolerant control [36]–[38]. Despite rich literature, existing model-based FD techniques are largely focused on systems with precisely known dynamics. The FD problem for more complex but realistic systems with unknown dynamics remains an open problem, especially, when the detection of "small" faults is concerned.

In the FD literature, small faults are typically referred to those faults whose magnitudes are smaller than those of system uncertainties (e.g., unmodeled dynamics or disturbances/noise), which normally appear in the early stage before the occurrence of larger faults [12], [13]. Knowing that early detection of small faults is critical for systems' safe operation and prompt maintenance, as well as avoiding larger faults and catastrophic consequences [14], [15], considerable research efforts have been devoted to investigate the associated problem of small FD (sFD) (see [12], [16], [42]). However, the research is still in its primitive stage, leaving many challenging issues that have yet to be adequately addressed. One of the most critical challenges lies in how to achieve sFD for nonlinear systems with unstructured uncertain dynamics, where distinguishing small faults from unmodeled system dynamics

Manuscript received May 15, 2019; revised August 14, 2019; accepted September 29, 2019. This work was supported in part by the National Science Foundation under Grant CMMI 1929729, and in part by the Division of Research and Economic Development through the University of Rhode Island under the Proposal Development Grant. This article was recommended by Associate Editor J. Q. Gan. *(Corresponding author: Chengzhi Yuan.)*

J. Zhang and C. Yuan are with the Department of Mechanical, Industrial and Systems Engineering, University of Rhode Island, Kingston, RI 02881 USA (e-mail: jingting_zhang@uri.edu; cyuan@uri.edu).

P. Stegagno and H. He are with the Department of Electrical, Computer, and Biomedical Engineering, University of Rhode Island, Kingston, RI 02881 USA (e-mail: pstegagno@uri.edu; he@ele.uri.edu).

C. Wang is with the School of Automation Science and Engineering, South China University of Technology, Guangzhou 510641, China (e-mail: wangcong@scut.edu.cn).

Color versions of one or more of the figures in this article are available online at http://ieeexplore.ieee.org.

Digital Object Identifier 10.1109/TCYB.2019.2945629

is a well-known difficulty. Some attempts have been made to overcome this difficulty. For instance, an adaptive dynamics estimation approach was proposed in [17] to monitor the system dynamics changes induced by faults, which, however, is limited to large faults (i.e., magnitude of faults larger than that of the system's modeling uncertainty). Zhang *et al.* [16] proposed an adaptive threshold-based sFD mechanism, which, however, leads to a rather restrictive detectability condition. In [12], an innovative sFD scheme was developed using the smallest residual principle (SRP). This scheme was demonstrated to be capable of dealing with small faults for nonlinear uncertain systems, but its effectiveness can be guaranteed only when the occurred faults strictly belong to a predefined fault set, leading to a possible FD misjudgment when a new fault occurs.

One promising solution to overcome the above challenge is to realize accurate identification/modeling of the associated system dynamics changes induced by faults. The adaptive neural network (NN) provides a powerful tool for this purpose. Some success along this article direction has been seen in recent years. For example, in [18], an online adaptive approximation-based FD method was developed by using adaptive NNs to estimate the fault dynamics. However, convergence of the associated NN weights to their optimal/true values is not analytically guaranteed, meaning that accurate modeling of fault dynamics is essentially not realized. Overcoming this issue hinges on the satisfaction of the so-called persistently exciting (PE) condition—a well-known technical challenge in the field of adaptive NN identification and control [19]. Recently, a deterministic learning (DL) theory was proposed in [20], which offers an elegant solution to the aforementioned issue. This theory adopts the following ingredients to enable accurate modeling using adaptive NNs: 1) employment of the localized radial basis function (RBF) networks; 2) satisfaction of a partial PE condition along a periodic or recurrent orbit; and 3) exponential convergence of partial RBF NN weights to their optimal/true values along the recurrent orbit. Consequently, locally accurate RBF NN identification of nonlinear system dynamics can be obtained, represented, and stored as a constant RBF NN model [21]. Applications of the DL theory to the sFD problem for nonlinear uncertain systems have been preliminarily explored in [12], [13], [22], and [42]. Several important issues are yet to be addressed, including how to deal with more stringent faults with frequently changing signs, how to accelerate the FD speed, how to avoid all those deficiencies induced by using the SRP (e.g., unable to detect new coming faults), and how to extend the methodology from continuous-time to discrete-time nonlinear uncertain systems.

In this article, we aim to address all of these issues by developing a new sFD approach based on the DL theory. Specifically, we seek to achieve sFD for discrete-time nonlinear systems with uncertain dynamics. First, to tackle the aforementioned problem that the small fault effects may be hidden within the system's uncertain dynamics, we propose a new discrete-time adaptive dynamics learning approach by leveraging the methodology from the continuous-time DL theory. This new approach enables locally accurate identification of the unknown system dynamics in the normal mode by using RBF NNs. Second, we propose designing a novel residual system by using a new mechanism of absolute measurements of the difference between the monitored system dynamics and the normal system dynamics (represented by a constant RBF NN model obtained from the learning phase). This residual system is able to monitor and estimate small changes of the system dynamics induced by small faults. Finally, based on the proposed residual system, an adaptive threshold is further designed for real-time sFD decision making. It is demonstrated through both rigorous analysis and extensive simulations that advanced over many existing FD techniques (e.g., [12], [17], and [23]), the proposed sFD scheme is able to remove the constraint on sign changes of associated fault functions, and avoid the use of the average L_1-norm for FD decision making, leading to a significantly relaxed detectability condition as well as shortened detection time.

The contributions of this article can be summarized in the following aspects.

1) We address the problem of sFD for nonlinear uncertain systems, where the fault is allowed to be small in the sense that their magnitudes could be smaller than those of the system's uncertain dynamics, and the associated system trajectories (states and inputs) could stay close to those in normal mode.
2) A novel discrete-time adaptive dynamics learning approach is proposed, enabling effective and accurate modeling of system's uncertain dynamics, which addresses the aforementioned technical challenge related to satisfaction of the PE condition in model-based FD research.
3) A new adaptive threshold-based sFD scheme is developed by embedding a novel mechanism of absolute measurements of dynamics difference into the sFD residual system, which advances the existing FD approaches (e.g., [12], [17], and [23]) with a significantly relaxed detectability condition and shortened detection time.

The remainder of this article is organized as follows. Section II provides some preliminary results and states the problem. The proposed adaptive dynamics learning approach is presented in Section III. Section IV presents the proposed sFD scheme and rigorous analysis on its performance. The simulation studies are shown in Section V. The conclusions are made in Section VI.

Notation: $\mathbb{R}$, $\mathbb{R}_+$, and $\mathbb{Z}_+$ denote, respectively, the set of real numbers, the set of positive real numbers, and the set of non-negative integers; $\mathbb{R}^{m\times n}$ denotes the set of $m \times n$ real matrices; and $\mathbb{R}^n$ denotes the set of $n \times 1$ real column vectors; and I_n denotes the $n \times n$ identity matrix. We denote the open ball $B_r := \{x \in \mathbb{R}^n : \|x\| < r\}$ with r being an arbitrary positive constant. $|\cdot|$ is the absolute value of a real number; $\|\cdot\|$ is the 2-norm of a vector or a matrix, that is, $\|x\| = (x^T x)^{(1/2)}$; $\|\cdot\|_1$ is the L_1-norm of a vector or a matrix, that is, $\|x(k)\|_1 = (1/K)\sum_{h=k-K}^{k-1} |x(h)|$ $(k \geq K > 1)$; and $\lceil a \rceil$ denotes the least integer greater than or equal to a real number a.

II. Preliminaries and Problem Formulation

A. Preliminaries

Consider the following discrete-time systems:

$$x(k+1) = f(x(k), k) + d(k) \tag{1}$$

where $k \in \mathbb{Z}_+$, $x(k) : \mathbb{Z}_+ \to \mathbb{R}^n$, $f(x(k), k) : \mathbb{R}^n \times \mathbb{Z}_+ \to \mathbb{R}^n$ is a single-valued function which is continuous in $x(k)$, and $d(k) : \mathbb{Z}_+ \to \mathbb{R}^n$ is also a single-valued function representing an unknown but bounded disturbance.

Lemma 1 [24]: If, for system (1), there exists a function $V(x(k), k)$ with continuous partial differences such that for $x(k)$ in a compact set $\Omega \subset \mathbb{R}^n$, $V(x(k), k)$ is positive definite (i.e., $V(x(k), k) > 0$), and $\Delta V(x(k), k) := V(x(k+1), k+1) - V(x(k), k) < 0$ for $\|x(k)\| > \chi$ with some constant $\chi > 0$ such that the ball of radius χ is contained in Ω, then the system is uniformly ultimately bounded (UUB) and the norm of the state is bounded within a neighborhood of χ.

Definition 1 [25]: A time-varying matrix sequence $\psi(k) : \mathbb{Z}_+ \to \mathbb{R}^{m\times n}$ is said to be PE if it is bounded and there exist some positive numbers $K_1 > 0$ and $\delta > 0$ such that $\sum_{k=K_0}^{K_0+K_1-1} \psi(k)\psi(k)^T \geq \delta I_m$, $\forall K_0 \in \mathbb{Z}_+$.

Consider the following linear time-varying system:

$$x(k+1) = A(k)x(k) + d(k) \tag{2}$$

where $A(k) : \mathbb{Z}_+ \to \mathbb{R}^{n\times n}$ is a matrix, and $d(k) : \mathbb{Z}_+ \to \mathbb{R}^n$ is an unknown but bounded disturbance, which satisfies $\|d(k)\| \leq d_M$ with a known positive constant bound d_M.

Lemma 2 [26]: Consider system (2). Assume $A(k) = I_n - \alpha\psi(k)\psi(k)^T$ with $\psi \in \mathbb{R}^n$, $\alpha \in \mathbb{R}$, $\alpha\psi(k)^T\psi(k) < \beta$ and $0 < \beta < 2$ for all $k \in \mathbb{Z}_+$, and d_M is small. If $\psi(k)$ is PE, then the state $x(k)$ will converge exponentially to a small neighborhood around the origin.

The RBF networks can be described by $f_{nn}(Z) = \sum_{i=1}^{N_n} w_i s_i(Z) = W^T S(Z)$ [27], where $Z \in \Omega_Z \subset \mathbb{R}^q$ is the input vector, $W = [w_1, \ldots, w_{N_n}]^T \in \mathbb{R}^{N_n}$ is the weight vector, N_n is the NN node number, and $S(Z) = [s_1(\|Z - \epsilon_1\|), \ldots, s_{N_n}(\|Z - \epsilon_{N_n}\|)]^T$, with $s_i(\cdot)$ being an RBF, and ϵ_i $(i = 1, 2, \ldots, N_n)$ being distinct points in state space. The Gaussian function $s_i(\|Z - \epsilon_i\|) = \exp[(-(Z - \epsilon_i)^T(Z - \epsilon_i))/(\eta_i^2)]$ is one of the most commonly used RBFs, where $\epsilon_i = [\epsilon_{i1}, \epsilon_{i2}, \ldots, \epsilon_{iq}]^T$ is the center of the receptive field and η_i is the width of the receptive field. The Gaussian function belongs to the class of localized RBFs in the sense that $s_i(\|Z - \epsilon_i\|) \to 0$ as $\|Z\| \to \infty$. It is easily seen that $S(Z)$ is bounded and there exists a real constant $S_M \in \mathbb{R}_+$ such that $\|S(Z)\| \leq S_M$ [19]. It has been shown in [28] that for any continuous function $f(Z) : \Omega_Z \to \mathbb{R}$, where $\Omega_Z \subset \mathbb{R}^q$ is a compact set, and for the NN approximator, where the node number N_n is sufficiently large, there exists an ideal constant weight vector W^*, such that for any $\epsilon^* > 0$, $f(Z) = W^{*T}S(Z) + \epsilon$, $\forall Z \in \Omega_Z$, where $|\epsilon| < \epsilon^*$ is the ideal approximation error. The ideal weight vector W^* is an "artificial" quantity required for analysis, and is defined as the value of W that minimizes $|\epsilon|$ for all $Z \in \Omega_Z \subset \mathbb{R}^q$, that is, $W^* := \arg\min_{W\in\mathbb{R}^{N_n}}\{\sup_{Z\in\Omega_Z}|f(Z) - W^T S(Z)|\}$. Moreover, based on the localization property of RBF NNs [19], for any bounded trajectory $Z(t)$ within the compact set Ω_Z, $f(Z)$ can be approximated by using a limited number of neurons located in a local region along the trajectory: $f(Z) = W_\zeta^{*T} S_\zeta(Z) + \epsilon_\zeta$, where ϵ_ζ is the approximation error, with $\epsilon_\zeta = O(\epsilon) = O(\epsilon^*)$, $S_\zeta(Z) = [s_{j1}(Z), \ldots, s_{j\zeta}(Z)]^T \in \mathbb{R}^{N_\zeta}$, $W_\zeta^* = [w_{j1}^*, \ldots, w_{j\zeta}^*]^T \in \mathbb{R}^{N_\zeta}$, $N_\zeta < N_n$, and the integers $j_i = j_1, \ldots, j_\zeta$ are defined by $|s_{j_i}(Z_p)| > \theta$ ($\theta > 0$ is a small positive constant) for some $Z_p \in Z(k)$. It is shown in [19] that for a localized RBF network $W^T S(Z)$ whose centers are placed on a regular lattice, almost any recurrent trajectory[1] $Z(k)$ can lead to the satisfaction of the PE condition of the regressor subvector $S_\zeta(Z)$. This result can be formally summarized in the following lemma.

Lemma 3 [29]: Consider any recurrent trajectory $Z(k) : \mathbb{Z}_+ \to \mathbb{R}^q$. $Z(k)$ remains in a bounded compact set $\Omega_Z \subset \mathbb{R}^q$, then for the RBF network $W^T S(Z)$ with centers placed on a regular lattice (large enough to cover compact set Ω_Z), the regressor subvector $S_\zeta(Z)$ consisting of RBFs with centers located in a small neighborhood of $Z(k)$ is PE.

B. Problem Formulation

Consider the following nonlinear discrete-time system:

$$\begin{aligned} x(k+1) = {} & f(x(k), u(k)) + v(x(k), u(k)) \\ & + \beta(k - k_0)\phi(x(k), u(k)) \end{aligned} \tag{3}$$

where $x = [x_1, \ldots, x_n]^T \in \mathbb{R}^n$ is the system state vector; $u = [u_1, \ldots, u_m]^T \in \mathbb{R}^m$ is the control input vector; $f(x, u) = [f_1(x, u), \ldots, f_n(x, u)]^T$, $v(x, u) = [v_1(x, u), \ldots, v_n(x, u)]^T$, $\phi(x, u) = [\phi_1(x, u), \ldots, \phi_n(x, u)]^T$ are nonlinear vector fields, with $f(x, u)$ representing the known nominal dynamics, $v(x, u)$ representing the modeling uncertainty, and $\phi(x, u)$ representing the deviation in system dynamics due to fault. $\beta(k-k_0)$ represents the fault time profile, where $\beta(k-k_0) = 0$ for $k < k_0$ and $\beta(k - k_0) = 1$ for $k \geq k_0$ with k_0 being the unknown fault occurrence time. In this article, system (3) is said to operate in the normal mode when no fault occurs (i.e., $0 < k < k_0$), and operate in the faulty mode when some fault occurs for $k \geq k_0$. To facilitate subsequent development, as typically adopted in [19], we assume that the system trajectories (x, u) in both the normal and faulty modes are recurrent.

Following similar definitions from [12] and [13], the fault considered in this article is small in the sense that: 1) the magnitude of the fault function $\phi(x, u)$ is allowed to be smaller than the magnitude of the modeling uncertainty $v(x, u)$, which means that the fault may be hidden within the modeling uncertainty and 2) the system trajectory under faulty mode [denoted by (x_f, u_f)] stays close to the under normal mode [denoted by (x_0, u_0)], that is

$$\begin{aligned} \operatorname{dist}\big((x_f, u_f), (x_0, u_0)\big) & := \max\big\{\min\big\{\big\|(x_f, u_f), (x_0, u_0)\big\|\big\}\big\} \\ & < d_\zeta \end{aligned} \tag{4}$$

where d_ζ is a constant number satisfying $0 < d_\zeta < d_\zeta^*$, where d_ζ^* is the size of the NN approximation region to be defined later.

[1]A recurrent trajectory represents a large set of periodic and periodic-like trajectories generated from linear/nonlinear dynamics systems. A detailed characterization of recurrent trajectories can be found in [19].

Given the above system setup, a novel adaptive dynamics learning-based sFD scheme will be proposed, which consists of two components.

1) *Accurate Adaptive Dynamics Learning:* Aiming to achieve locally accurate identification of unknown system dynamics $v(x, u)$ when the system is in normal mode.
2) *sFD:* Aiming to realize rapid detection of occurrence of small faults for system (3).

III. System Uncertain Dynamics Identification

This section will first present a novel adaptive dynamics learning approach. Consider the normal system from (3)

$$x(k+1) = f(x(k), u(k)) + v(x(k), u(k)) \tag{5}$$

where $v(x, u)$ is the system unknown dynamics to be accurately identified. According to the RBF NN approximation theory as presented in Section II-A, we know that there exists an ideal constant NN weight vector $W^* = [W_1^*, \ldots, W_n^*] \in \mathbb{R}^{N_n \times n}$ (N_n is the number of NN nodes) such that

$$v_i(x,\ u) = W_i^{*T} S(x,\ u) + \epsilon_i, \quad i = 1, \ldots, n \tag{6}$$

where $S(x,\ u) : \mathbb{R}^n \times \mathbb{R}^m \to \mathbb{R}^{N_n}$ is a smooth RBF vector and ϵ_i is the associated ideal estimation error satisfying $|\epsilon_i| < \epsilon^*$ with ϵ^* being a positive constant that can be made arbitrarily small given a sufficiently large N_n. Then, motivated by [30], we propose the following adaptive dynamics estimator to identify the unknown dynamics $v(x, u)$ of (5):

$$\begin{aligned}\hat{x}_i(k+1) &= a_i\big(\hat{x}_i(k) - x_i(k)\big) + f_i(x(k), u(k)) \\ &\quad + \hat{W}_i^T(k) S(x(k), u(k)), \quad \forall i = 1, \ldots, n\end{aligned} \tag{7}$$

where $\hat{x}_i \in \mathbb{R}$ is the estimator state, x_i is the state of system (5), and a_i is a positive design constant. $\hat{W}_i \in \mathbb{R}^{N_n}$ is the estimate of W_i^*, which is updated in real time using

$$\hat{W}_i(k+1) = \hat{W}_i(k) - c_i \tilde{x}_i(k+1) S(x(k), u(k)) \tag{8}$$

with c_i being a positive constant and $\tilde{x}_i(k) := \hat{x}_i(k) - x_i(k)$, whose dynamics can be deduced from (5)–(7)

$$\tilde{x}_i(k+1) = a_i \tilde{x}_i(k) + \tilde{W}_i^T(k) S(x(k), u(k)) - \epsilon_i \tag{9}$$

where $\tilde{W}_i(k) := \hat{W}_i(k) - W_i^*$.

In the following theorem, we denote the trajectory generated from the normal system (5) as φ^0. Following [19], we use $(\cdot)_\zeta$ and $(\cdot)_{\bar{\zeta}}$ to represent the parts of $(\cdot)$ related to the regions close to and away from the trajectory φ^0, respectively.

Theorem 1: Consider the adaptive learning system consisting of the plant (5), the estimators (7), and the NN weight updating law (8). Given recurrent orbits φ^0, with initial conditions $(x(0),\ u(0)) \in \Omega_0$ (where Ω_0 is a compact set) and $\hat{W}_i(0) = 0$ ($i = 1, \ldots, n$), if the associated coefficients a_i in (7) and c_i in (8) are chosen to satisfy

$$0 < a_i < \frac{\sqrt{5} - 1}{2}, \qquad 0 < c_i < \frac{1}{S_M^2 (2 + a_i)} \tag{10}$$

with S_M being the upper bound of $\|S(x,\ u)\|$, then we have the following.

1) All signals in the system remain UUB; the estimation error $\tilde{x}_i$ converges to a small neighborhood around the origin; and the local NN weight $\hat{W}_{i_\zeta}$ converges to a small neighborhood of its associated ideal value $W_{i_\zeta}^*$ along the trajectory φ^0 for all $i = 1, \ldots, n$.
2) A locally accurate approximation for the system uncertainty $v_i(x,\ u)$ in (5) can be obtained by $\hat{W}_i^T S(x,\ u)$ as well as $\bar{W}_i^T S(x,\ u)$ along the trajectory φ^0 for all $i = 1, \ldots, n$, where

$$\bar{W}_i := \frac{1}{K_2} \sum_{k=K_1}^{K_1+K_2-1} \hat{W}_i(k) \tag{11}$$

with $k \in [K_1,\ K_1 + K_2 - 1]$ representing a time segment after the transient process.

Proof: 1) From (8) and (9), we obtain

$$\begin{aligned}\tilde{W}_i(k+1) &= \big(I - c_i S(x(k), u(k)) S^T(x(k), u(k))\big)\tilde{W}_i(k) \\ &\quad + c_i \epsilon_i S(x(k), u(k)) - c_i a_i \tilde{x}_i(k) S(x(k), u(k)) \\ \tilde{x}_i(k+1) &= a_i \tilde{x}_i(k) + \tilde{W}_i^T(k) S(x(k), u(k)) - \epsilon_i.\end{aligned} \tag{12}$$

Consider a Lyapunov function candidate for (12)

$$V_i(k) = \tilde{x}_i^2(k) + \frac{1}{c_i} \tilde{W}_i^T(k) \tilde{W}_i(k). \tag{13}$$

The forward difference of (13) along (12) is given as

$$\begin{aligned}\Delta V_i &= V_i(k+1) - V_i(k) \\ &= \Big(a_i^2 - 1 + c_i a_i^2 S^T(x(k), u(k)) S(x(k), u(k))\Big)\tilde{x}_i^2(k) \\ &\quad + \big(c_i S^T(x(k), u(k)) S(x(k), u(k)) - 1\big) \\ &\quad \times \big(\tilde{W}_i^T(k) S(x(k), u(k))\big)^2 \\ &\quad - 2c_i S^T(x(k), u(k)) S(x(k), u(k)) \epsilon_i \tilde{W}_i^T(k) S(x(k), u(k)) \\ &\quad + 2c_i a_i S^T(x(k), u(k)) S(x(k), u(k)) \tilde{x}_i \\ &\quad \times (k) \tilde{W}_i^T(k) S(x(k), u(k)) \\ &\quad - \big(2a_i + 2c_i a_i S^T(x(k), u(k)) S(x(k), u(k))\big)\epsilon_i \tilde{x}_i(k) \\ &\quad + \big(1 + c_i S^T(x(k), u(k)) S(x(k), u(k))\big)\epsilon_i^2.\end{aligned} \tag{14}$$

Noting that $c_i > 0$, $a_i > 0$, and $S^T(x, u) S(x, u) \geq 0$, it is easy to obtain the following inequalities:

$$\begin{aligned}&-2c_i S^T(x, u) S(x, u) \epsilon_i \tilde{W}_i^T S(x, u) \\ &\quad \leq c_i S^T(x, u) S(x, u) \Big(\epsilon_i^2 + \big(\tilde{W}_i^T S(x, u)\big)^2\Big) \\ &2c_i a_i S^T(x, u) S(x, u) \tilde{x}_i \tilde{W}_i^T S(x, u) \\ &\quad \leq c_i a_i S^T(x, u) S(x, u) \Big(\tilde{x}_i^2 + \big(\tilde{W}_i^T S(x, u)\big)^2\Big).\end{aligned} \tag{15}$$

Substituting (15) into (14) results in

$$\begin{aligned}\Delta V_i &\leq -\lambda_1 \tilde{x}_i^2 - \lambda_2 \big(\tilde{W}_i^T S(x, u)\big)^2 - 2\lambda_3 \epsilon_i \tilde{x}_i + \lambda_4 \epsilon_i^2 \\ &= -\lambda_1 \left(\tilde{x}_i^2 + \frac{2\lambda_3}{\lambda_1} \epsilon_i \tilde{x}_i - \frac{\lambda_4}{\lambda_1} \epsilon_i^2\right) - \lambda_2 \big(\tilde{W}_i^T S(x, u)\big)^2\end{aligned} \tag{16}$$

where $\lambda_1 := 1 - a_i^2 - (a_i^2 + a_i) c_i S^T(x, u) S(x, u)$, $\lambda_2 := 1 - (2 + a_i) c_i S^T(x, u) S(x, u)$, $\lambda_3 := a_i + c_i a_i S^T(x, u) S(x, u)$, and $\lambda_4 := 1 + 2c_i S^T(x, u) S(x, u)$. Recalling that $S^T(x, u) S(x, u) \leq$

S_M^2, combined with (10), we have: $\lambda_1 > 0$, $\lambda_2 > 0$, $\lambda_3 > 0$, and $\lambda_4 > 0$. Then, according to (16), $\Delta V_i < 0$ as long as

$$\tilde{x}_i^2 + \frac{2\lambda_3}{\lambda_1}\tilde{x}_i\epsilon_i - \frac{\lambda_4}{\lambda_1}\epsilon_i^2 > 0 \tag{17}$$

which is equivalent to

$$|\tilde{x}_i| > |\epsilon_i|\frac{\lambda_3 + \sqrt{\lambda_3^2 + \lambda_1\lambda_4}}{\lambda_1}. \tag{18}$$

Similarly, completing the squares for $\tilde{x}_i$ using (16) yields

$$\Delta V_i \le -\lambda_1\left(\tilde{x}_i + \frac{\lambda_3}{\lambda_1}\epsilon_i\right)^2 - \lambda_2\big(\tilde{W}_i^T S(x,u)\big)^2 + \frac{\lambda_3^2 + \lambda_1\lambda_4}{\lambda_1}\epsilon_i^2. \tag{19}$$

Then, $\Delta V_i < 0$ holds under condition (10) and

$$\big|\tilde{W}_i^T S(x,u)\big| > |\epsilon_i|\sqrt{\frac{\lambda_3^2 + \lambda_1\lambda_4}{\lambda_1\lambda_2}}. \tag{20}$$

Consequently, according to Lemma 1, it can be concluded that $\tilde{x}_i$ and $\tilde{W}_i^T S(x,u)$ are UUB, and all system signals in (12) remain UUB. In addition, noting that $|\epsilon_i| < \epsilon^*$ in (6) and (18) implies that given an arbitrary constant ρ satisfying $\rho \ge |\epsilon_i|[(\lambda_3+\sqrt{\lambda_3^2 + \lambda_1\lambda_4})/(\lambda_1)] = O(\epsilon^*)$, there must exist a finite K such that for all $k > K$, $|\tilde{x}_i(k)| \le \rho$, that is, $\tilde{x}_i(k) = O(\epsilon^*)$. Since ϵ^* can be made arbitrary small, it implies that $\tilde{x}_i$ will converge to a small neighborhood around the origin.

Moreover, by using the localization property of Gaussian RBF NNs, along the system trajectory φ^0, the dynamics of $\tilde{W}_i$ in (12) yields for all $i = 1, \ldots, n$ that

$$\begin{aligned}\tilde{W}_{i_\zeta}(k+1) = &\Big(I - c_i S_\zeta(x(k),u(k)) S_\zeta^T(x(k),u(k))\Big)\tilde{W}_{i_\zeta}(k)\\ &+ c_i\epsilon_{i_\zeta} S_\zeta(x(k),u(k)) - c_i a_i \tilde{x}_i(k) S_\zeta(x(k),u(k)).\end{aligned} \tag{21}$$

Since the trajectory of the NN input (x, u) is recurrent, $S_\zeta(x, u)$ satisfies PE according to Lemma 3. Note that $S_\zeta(x, u)$ is bounded, ϵ_{i_ζ} and $\tilde{x}_i$ are arbitrarily small and c_i can be selected to be small; thus, $\|c_i\epsilon_{i_\zeta} S_\zeta(x,u) - c_i a_i \tilde{x}_i S_\zeta(x,u)\|$ can be made arbitrarily small. Furthermore, under condition (10), we have $0 < c_i S_\zeta(x,u) S_\zeta^T(x,u) < 1$. Then according to Lemma 2, the error $\tilde{W}_{i_\zeta} = \hat{W}_{i_\zeta} - W_{i_\zeta}^*$ is guaranteed to converge exponentially to a small neighborhood around the origin. Thus, it is proved that along the system trajectory φ^0, the weight $\hat{W}_{i_\zeta}$ will converge exponentially to a small neighborhood of its ideal value $W_{i_\zeta}^*$.

2) Based on the localization property of RBF NNs, convergence of $\hat{W}_{i_\zeta}$ to a small neighborhood of $W_{i_\zeta}^*$ implies that along the trajectory φ^0, the system uncertain dynamics $v_i(x, u)$ $(i = 1, \ldots, n)$ in (5) can be rewritten as

$$\begin{aligned} v_i(x,u) &= W_{i_\zeta}^{*T} S_\zeta(x,u) + \epsilon_{i_\zeta}\\ &= \hat{W}_{i_\zeta}^T S_\zeta(x,u) - \tilde{W}_{i_\zeta}^T S_\zeta(x,u) + \epsilon_{i_\zeta}\\ &= \hat{W}_{i_\zeta}^T S_\zeta(x,u) + \epsilon_{i_{\zeta_1}} = \bar{W}_{i_\zeta}^T S_\zeta(x,u) + \epsilon_{i_{\zeta_2}} \end{aligned} \tag{22}$$

where $\epsilon_{i_{\zeta_1}} = \epsilon_{i_\zeta} - \tilde{W}_{i_\zeta}^T S_\zeta(x,u) = O(\epsilon_{i_\zeta}) = O(\epsilon^*)$, which is small due to the exponential convergence of $\tilde{W}_{i_\zeta}$ to a small neighborhood around origin; $\bar{W}_{i_\zeta}$ is the corresponding submatrix of $\bar{W}_i$ defined in (11) along the trajectory φ^0; and $\epsilon_{i_{\zeta_2}}$ is the approximation error using $\bar{W}_{i_\zeta}^T S_\zeta(x,u)$ and satisfies $\epsilon_{i_{\zeta_2}} = O(\epsilon_{i_{\zeta_1}}) = O(\epsilon^*)$ after the transient process [19].

In addition, for the neurons with centers far away from the trajectory φ^0, $|S_{\bar{\zeta}}(x,u)|$ would become very small due to the localization property of RBFs. In this case, the neural weights $\hat{W}_{i_{\bar{\zeta}}}$ would be only slightly updated and stay close to zero under the NN adaptation law (8) with $\hat{W}_i(0) = 0$. Then both $\hat{W}_{i_{\bar{\zeta}}}$ and $\hat{W}_{i_{\bar{\zeta}}}^T S_{\bar{\zeta}}(x,u)$, as well as $\bar{W}_{i_{\bar{\zeta}}}$ and $\bar{W}_{i_{\bar{\zeta}}}^T S_{\bar{\zeta}}(x,u)$, would remain very small. Consequently, along the trajectory φ^0, the system uncertainty $v_i(x,u)$ can be represented as

$$\begin{aligned} v_i(x,u) &= \hat{W}_{i_\zeta}^T S_\zeta(x,u) + \epsilon_{i_{\zeta_1}}\\ &= \hat{W}_{i_\zeta}^T S_\zeta(x,u) + \hat{W}_{i_{\bar{\zeta}}}^T S_{\bar{\zeta}}(x,u) + \epsilon_{i_1}\\ &= \hat{W}_i^T S(x,u) + \epsilon_{i_1} \end{aligned} \tag{23}$$

where $\epsilon_{i_1} = \epsilon_{i_{\zeta_1}} - \hat{W}_{i_{\bar{\zeta}}}^T S_{\bar{\zeta}}(x,u) = O(\epsilon^*)$.

Similarly, we have

$$\begin{aligned} v_i(x,u) &= \bar{W}_{i_\zeta}^T S_\zeta(x,u) + \epsilon_{i_{\zeta_2}}\\ &= \bar{W}_{i_\zeta}^T S_\zeta(x,u) + \bar{W}_{i_{\bar{\zeta}}}^T S_{\bar{\zeta}}(x,u) + \epsilon_{i_2}\\ &= \bar{W}_i^T S(x,u) + \epsilon_{i_2} \end{aligned} \tag{24}$$

where $\epsilon_{i_2} = \epsilon_{i_{\zeta_2}} - \bar{W}_{i_{\bar{\zeta}}}^T S_{\bar{\zeta}}(x,u) = O(\epsilon^*)$.

Consequently, according to (23) and (24), we have that for all $i = 1, \ldots, n$, a locally accurate approximation of the system uncertainty $v_i(x,u)$ can be obtained by $\hat{W}_i^T S(x,u)$ as well as $\bar{W}_i^T S(x,u)$ along the trajectory φ^0. ∎

Remark 1: Since $S(Z)$ consists of N_n number of Gaussian function elements, a conservative selection for the value of S_M in (10) could be $\sqrt{N_n}$. For a tighter upper bound of $\|S(Z)\|$, one can refer to [33].

Remark 2: Note that the proposed adaptive dynamics learning scheme (7) and (8) differs from those proposed in [30] and [34] in two important aspects.

1) The system dynamics to be identified are different. Yuan and Wang [30] and Wu *et al.* [34] considered identifying continuous-time dynamics using sampling data; while this article considers learning unknown nonlinear dynamics in a general discrete-time form.
2) The methods for proving system stability and parameter convergence are different. Wu *et al.* [34] incorporated small-gain theorem with Lyapunov functions; while this article proposes a relatively simpler and more compact proof by utilizing only the Lyapunov stability method.

Remark 3: The proof of Theorem 1 demonstrates that system (12) is UUB, and there exists a finite time K such that the error signals $\tilde{x}_i$ and $\tilde{W}_{i_\zeta}$ will converge to a small bounded neighborhood around the origin. Note that these results are sufficient to ensure the stability and convergence properties of the proposed adaptive learning system, establishing explicit relationships between K and the error bounds is not mandatory for its effective implementation. Nevertheless, addressing this problem is meaningful, which although is out of the scope of this article. The promising methods for future research along this direction can be found in [25], [30], and [35].

According to (24), for $(x_0, u_0) \in \varphi^0$, the RBF NN $\bar{W}_i^T S(x_0, u_0)$ with constant weights $\bar{W}_i$ defined in (11) provides locally accurate approximation of the system uncertain dynamics $v_i(x_0, u_0)$ with the approximation error ϵ_{i_2} satisfying $\epsilon_{i_2} = O(\epsilon^*)$. Based on this, one can always prespecify a small constant number ε^* such that $|\epsilon_{i_2}| < \varepsilon^*$ by using a sufficiently large number of neurons. Furthermore, according to [31], $\bar{W}_i^T S(x_0, u_0)$ has a certain ability of generalization in the sense that the locally accurate approximation of $\bar{W}_i^T S(x_0, u_0)$ for $v_i(x_0, u_0)$ is achieved in a local region Ω_ζ^0 along the trajectory φ^0, where Ω_ζ^0 can be defined as

$$\Omega_\zeta^0 := \left\{(x, u)|\mathrm{dist}\Big((x, u), \varphi^0\Big) < d_\zeta^*\right\} \tag{25}$$

with $d_\zeta^* > 0$ characterizing the size of the NN approximation region. Such a generalization ability indicates that if $(x, u) \in \Omega_\zeta^0$, we have that $v_i(x, u)$ can be locally accurately approximated by $\bar{W}_i^T S(x, u)$, that is, $v_i(x, u) = \bar{W}_i^T S(x, u) + \epsilon_{i_3}$ for all $i = 1, \ldots, n$, where the approximation error ϵ_{i_3} is bounded by $|\epsilon_{i_3}| < \xi^*$ with ξ^* depending on d_ζ^*. Based on this, with the small fault assumption given in (4), a faulty trajectory (x_f, u_f) generated from system (3) satisfies $\mathrm{dist}((x_f, u_f), (x_0, u_0)) < d_\zeta^*$, implying that $(x_f, u_f) \in \Omega_\zeta^0$. As a result, we have

$$v_i\big(x_f, u_f\big) = \bar{W}_i^T S\big(x_f, u_f\big) + \epsilon_{i_3}, \quad \forall i = 1, \ldots, n. \tag{26}$$

In summary, with (24) and (26), we rewrite the RBF NN approximation of the system uncertainty $v_i(x, u)$ in the following form for all $i = 1, \ldots, n$ and $(x, u) \in \Omega_\zeta^0$:

$$v_i(x, u) = \bar{W}_i^T S(x, u) + \xi_i \tag{27}$$

where (x, u) is the system trajectory generated from (3), and ξ_i is the generalized approximation error with $|\xi_i| = |\epsilon_{i_2}| < \varepsilon^*$ for $(x, u) = (x_0, u_0)$ and $|\xi_i| = |\epsilon_{i_3}| < \xi^*$ for $(x, u) = (x_f, u_f)$.

IV. Small Fault Detection

Based on the results from the previous section, this section will present a novel sFD scheme and its performance analysis.

A. Residual System Design and Detection Scheme

Recall the monitored system from (3) as follows:

$$\begin{aligned} x(k+1) =& f(x(k), u(k)) + v(x(k), u(k)) \\ &+ \beta(k-k_0)\phi(x(k), u(k)) \end{aligned} \tag{28}$$

where k_0 is the fault occurrence time. For $0 \le k < k_0$, system (28) operates in the normal mode, that is, $(x, u) = (x_0, u_0)$, and for $k \ge k_0$, the system operates in the faulty mode, that is, $(x, u) = (x_f, u_f)$. We propose the following residual system embedded with a novel mechanism of absolute measurements of dynamics difference:

$$\begin{aligned} e_i(k) =& b_i e_i(k-1) + \big|\bar{W}_i^T S(x(k-1), u(k-1)) \\ &+ f_i(x(k-1), u(k-1)) - x_i(k)\big|, \quad i = 1, \ldots, n \end{aligned} \tag{29}$$

where e_i is the state of the residual system and x_i is the state of the monitored system (28); $f_i(x, u)$ is the known nominal dynamics of (28); b_i is a design parameter satisfying $0 \le b_i < 1$; and $\bar{W}_i^T S(x, u)$ is a constant RBF NN obtained from the identification phase.

Remark 4: According to (27), $\bar{W}_i^T S(x(k-1), u(k-1)) + f_i(x(k-1), u(k-1))$ provides a locally accurate approximation of $x_i(k) = f_i(x(k-1), u(k-1)) + v_i(x(k-1), u(k-1))$. So, $|\bar{W}_i^T S(x(k-1), u(k-1)) + f_i(x(k-1), u(k-1)) - x_i(k)|$ in (29) essentially characterizes the absolute difference between the monitored system dynamics in (28) and the normal system dynamics.

Based on (29), an adaptive threshold will be further developed for real-time sFD decision making. Such an adaptive threshold is a time-varying function that will bound the residual signal of (29) [i.e., $e_i(k)$] at every time instant k if the system is operating in normal mode. To this end, from (27) and (28), we can rewrite (29) as

$$\begin{aligned} e_i(k) = b_i e_i(k-1) + |\beta(k-1-k_0)\phi_i(x(k-1), u(k-1)) \\ + \xi_i|. \end{aligned} \tag{30}$$

Choosing $e_i(0) = 0$, the solution to (30) can be obtained as

$$e_i(k) = \sum_{h=0}^{k-1} b_i^{k-1-h} |\beta(h-k_0)\phi_i(x(h), u(h)) + \xi_i| \tag{31}$$

which shows that the fault effect can be directly reflected by the residual e_i (with a weighting factor b_i).

When system (28) operates in normal mode, we have $\beta(k-k_0)\phi_i(x(k), u(k)) = 0$. Noting that $|\xi_i| = |\epsilon_{i_2}| < \varepsilon^*$ from (27), we can further obtain the following result from (31):

$$e_i(k) = \sum_{h=0}^{k-1} b_i^{k-1-h} \big|\epsilon_{i_2}\big| < \sum_{h=0}^{k-1} b_i^{k-1-h} \varepsilon^* = \frac{\big(1-b_i^k\big)\varepsilon^*}{1-b_i} \tag{32}$$

for $0 < k \le k_0$. Consequently, the adaptive threshold, denoted by $\bar{e}_i$, can be specified as

$$\bar{e}_i(k) := \frac{\big(1-b_i^k\big)\varepsilon^*}{1-b_i}, \quad i = 1, \ldots, n. \tag{33}$$

Recall that b_i is the design parameter, and ε^* is the desired accuracy level of the NN approximation as defined in (27), which can be prespecified by setting a sufficiently large number of neurons in the identification phase (as will be illustrated in Section V).

Based on this, we are ready to present the sFD decision-making scheme. The key idea is illustrated in Fig. 1. If no fault occurs in the monitored system (28), $e_i(k)$ $(i = 1, \ldots, n)$ in (29) will remain small such that $e_i(k) \le \bar{e}_i(k)$. Whenever this condition is violated, it indicates that the monitored system is no longer operating in normal mode and there must exist some faults in it. We formalize this idea as follows.

sFD Decision Scheme: Compare $e_i(k)$ of the residual system (29) with the adaptive threshold $\bar{e}_i(k)$ in (33) for each $i = 1, \ldots, n$. If there exists a finite time $k_d > 0$ and at least one component $i \in \{1, \ldots, n\}$ such that $e_i(k_d) > \bar{e}_i(k_d)$, then occurrence of a fault is deduced at time k_d.

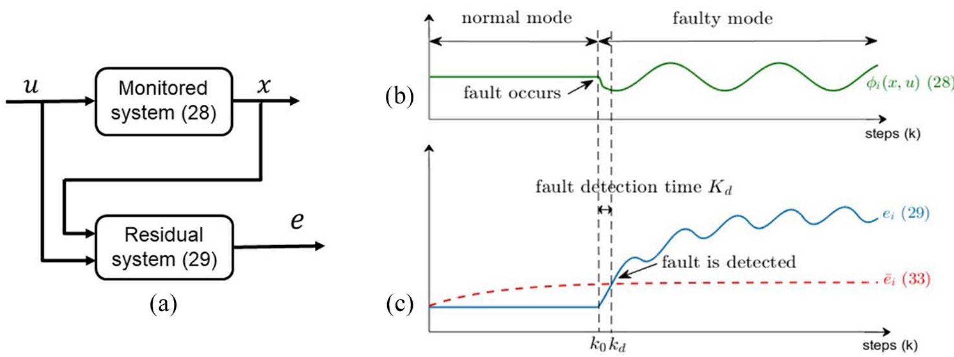

Fig. 1. Schematic of the proposed adaptive threshold-based sFD scheme. (a) Architecture of the sFD system. (b) Illustrative time profile of fault function $\phi_i(x, u)$. (c) Illustrative time profiles of residual e_i and adaptive threshold $\bar{e}_i$. Fault occurs at time k_0 and is detected at time k_d when $e_i(k) > \bar{e}_i(k)$, the corresponding FD time is $K_d = k_d - k_0$.

Remark 5: The proposed adaptive threshold $\bar{e}_i$ ($i = 1, \ldots, n$) in (33) is tight, that is, it can be made small due to its dependency of ε^*.

Remark 6: Existing FD schemes as proposed in [17] and [23] are not capable of coping with faults that have frequently changing signs. This is because the residual systems designed therein are all based on direct (instead of absolute) measurements of the system dynamics difference. This leads to that if the occurred fault function frequently changes its sign, the difference of the system dynamics between the normal mode and the faulty mode could be offset, making it difficult to observe fault occurrence from the associated residual signal which will stay close to zero. This issue is overcome with our proposed residual system (29) by using absolute measurement of dynamics difference. Specifically, it is noted from (31) that even the fault function $\phi_i(x, u)$ has frequently changing signs, its accumulated effects would not be offset and thus e_i will not approach to zero. This demonstrates the superiority of our sFD scheme in dealing with more general and stringent faults. Another important advantage of our method lies in that e_i can be used directly for decision making without any tedious additional signal processing (e.g., the average L_1-norm processing as adopted in [12], [13], and [22]).

Remark 7: Existing NN-based FD schemes (e.g., [17] and [23]) cannot guarantee accurate approximation of fault dynamics. As a result, they usually require the magnitude of occurred fault to be larger enough than that of the system uncertainty, which is not always feasible under the sFD context. This issue is addressed with our new sFD approach, which ensures accurate RBF NN approximation of uncertain system dynamics. In addition, since the system uncertainty can be accurately approximated, stored, and represented in terms of constant RBF NN models, and further reused for FD, our method does not need any further online parameter estimation during the detection process, which significantly reduces the computational burden and thus enhances the FD efficiency.

Remark 8: An important class of existing sFD schemes is based on the SRP (e.g., [12] and [22]), which suffers from a critical drawback that only those faults belonging to a predefined fault set can be detected, leading to a possible FD misjudgment when a new coming fault occurs. As such, in order to enhance their detection capabilities, a sufficiently large number of possible faults usually need to be identified and included in the predefined fault set, resulting in a large number of estimators (residual systems) needed for online sFD. However, this drawback is overcome in our sFD scheme, that is, the predefined fault set is not required and only one estimator needs to be implemented for online sFD. This is due to the adoption of an adaptive threshold mechanism instead of the SRP. Moreover, with our scheme, except the system uncertain dynamics in normal mode, any fault dynamics does not need to be identified. This distinguishes our method from the sFD schemes in [12] and [22], where all the predefined fault dynamics need to be identified in the learning phase.

B. Fault Detectability Condition and Detection Time

To analyze the performance of the proposed sFD scheme, we denote the absolute FD time as k_d, and the FD time K_d as $K_d = k_d - k_0$. We first study the detectability condition.

Theorem 2: Consider the monitored system (28) and the sFD system consisting of (29) and (33). Under the proposed sFD scheme, if for at least one component $i \in \{1, \ldots, n\}$, there exists a finite time $k_f > k_0$ such that

$$\sum_{h=k_0}^{k_f-1} b_i^{k_f-1-h} |\phi_i(x(h), u(h))| > \frac{\xi^* + \varepsilon^*}{1 - b_i} \tag{34}$$

then $e_i(k_f) > \bar{e}_i(k_f)$ [where $\bar{e}_i$ is defined in (33)] holds and the fault will be detected at k_f, that is, $k_d = k_f$.

Proof: Consider (30) and (31), the residual signal $e_i(k_f)$ (for $k_f > k_0$) can be described by

$$e_i\big(k_f\big) = \sum_{h=0}^{k_0-1} b_i^{k_f-1-h} |\xi_i| + \sum_{h=k_0}^{k_f-1} b_i^{k_f-1-h} |\phi_i(x(h), u(h)) + \xi_i|. \tag{35}$$

Noting that $b_i \geq 0$ and for $k \geq k_0$, $(x, u) = (x_f, u_f)$ and $|\xi_i| = |\epsilon_{i_3}| < \xi^*$ from (27), by the triangular inequality, we have

$$
\begin{aligned}
e_i(k_f) &\geq \sum_{h=k_0}^{k_f-1} b_i^{k_f-1-h}\left|\phi_i(x(h), u(h)) + \epsilon_{i_3}\right| \\
&\geq \sum_{h=k_0}^{k_f-1} b_i^{k_f-1-h}|\phi_i(x(h), u(h))| - \sum_{h=k_0}^{k_f-1} b_i^{k_f-1-h}\left|\epsilon_{i_3}\right| \\
&> \sum_{h=k_0}^{k_f-1} b_i^{k_f-1-h}|\phi_i(x(h), u(h))| - \sum_{h=k_0}^{k_f-1} b_i^{k_f-1-h}\xi^* \\
&= \sum_{h=k_0}^{k_f-1} b_i^{k_f-1-h}|\phi_i(x(h), u(h))| - \frac{\left(1 - b_i^{k_f-k_0}\right)\xi^*}{1 - b_i} \\
&> \sum_{h=k_0}^{k_f-1} b_i^{k_f-1-h}|\phi_i(x(h), u(h))| - \frac{\xi^*}{1 - b_i}
\end{aligned}
$$

which yields $e_i(k_f) > \bar{e}_i(k_f) = ([(1 - b_i^{k_f})\varepsilon^*]/[1 - b_i])$ under (34). ■

Remark 9: The detectability condition (34) shows that for some $i \in \{1, \ldots, n\}$, if the magnitude of the fault function (i.e., $|\phi_i(x(k), u(k))|$) accumulating over a certain time interval $[k_0, k_f - 1]$ (i.e., $\sum_{h=k_0}^{k_f-1} b_i^{k_f-1-h}|\phi_i(x(h), u(h))|$) is large enough, then the occurred fault can be detected at time k_f. This condition is not restrictive because the associated lower bound $[(\xi^* + \varepsilon^*)/(1 - b_i)]$ is depending on ε^* and ξ^* (which can be made small). In addition, even the fault function $\phi_i(x(k), u(k))$ has frequently changing signs, condition (34) could still be satisfied due to the absolute measurements of $\phi_i(x(k), u(k))$. This is consistent with our discussions in Remark 6.

We further study the FD time, that is, how to estimate the upper bound of FD time K_d.

Theorem 3: Consider the monitored system (28) and the sFD system consisting of (29) and (33). Under the proposed sFD scheme, if for some $i \in \{1, \ldots, n\}$, there exists at most T_i number of separate time instants $k_{i,t} \in [k_0, k_d - 1]$ $(t = 1, \ldots, T_i)$ such that

$$\left|\phi_i\left(x\left(k_{i,t}\right), u\left(k_{i,t}\right)\right)\right| < \mu_i \tag{36}$$

where $\mu_i > \xi^*+\varepsilon^*$ and $T_i < \log_{b_i}[(\xi^*+\varepsilon^*)/\mu_i]$, then $e_i(k_d) > \bar{e}_i(k_d)$ [where $\bar{e}_i$ is defined in (33)] holds and the fault will be detected at k_d. The upper bound on K_d is given by

$$\bar{K}_d = \min_{i=1,2,\ldots,n}\left\{\left\lceil \log_{b_i}\frac{b_i^{T_i}\mu_i - \varepsilon^* - \xi^*}{\mu_i - \xi^*}\right\rceil\right\}. \tag{37}$$

Proof: Consider (30) and (31), the residual signal $e_i(k_d)$ (for $k_d > k_0$) can be described by

$$e_i(k_d) = \sum_{h=0}^{k_0-1} b_i^{k_d-1-h}|\xi_i| + \sum_{h=k_0}^{k_d-1} b_i^{k_d-1-h}|\phi_i(x(h), u(h)) + \xi_i|. \tag{38}$$

Noting that for $k \geq k_0$, $(x, u) = (x_f, u_f)$, $|\xi_i| = |\epsilon_{i_3}| < \xi^*$ according to (27), and $b_i \geq 0$, we obtain

$$
\begin{aligned}
e_i(k_d) &\geq \sum_{h=k_0}^{k_d-1} b_i^{k_d-1-h}\left|\phi_i(x(h), u(h)) + \epsilon_{i_3}\right| \\
&\geq \sum_{h=k_0}^{k_d-1} b_i^{k_d-1-h}\left(|\phi_i(x(h), u(h))| - |\epsilon_{i_3}|\right) \\
&> \sum_{h=k_0}^{k_d-1} b_i^{k_d-1-h}|\phi_i(x(h), u(h))| - \sum_{h=k_0}^{k_d-1} b_i^{k_d-1-h}\xi^* \\
&= \sum_{h=k_0}^{k_d-1} b_i^{k_d-1-h}|\phi_i(x(h), u(h))| - \frac{\left(1 - b_i^{k_d-k_0}\right)\xi^*}{1 - b_i}.
\end{aligned}
\tag{39}
$$

Equation (36) implies that there exists at least $k_d - k_0 - T_i$ number of time instants $k_{i,\bar{t}}$ $(k_{i,\bar{t}} \in [k_0, k_d-1]/\{k_{i,t}\})$ satisfying $|\phi_i(x(k_{i,\bar{t}}), u(k_{i,\bar{t}}))| \geq \mu_i$. With $0 \leq b_i < 1$, we have

$$
\begin{aligned}
&\sum_{h=k_0}^{k_d-1} b_i^{k_d-1-h}|\phi_i(x(h), u(h))| \geq \sum_{h=k_{i,\bar{t}}} b_i^{k_d-1-h}|\phi_i(x(h), u(h))| \\
&\geq \sum_{h=k_{i,\bar{t}}} b_i^{k_d-1-h}\mu_i \geq \sum_{h=k_0}^{k_d-T_i-1} b_i^{k_d-1-h}\mu_i \\
&= \frac{\left(b_i^{T_i} - b_i^{k_d-k_0}\right)\mu_i}{1 - b_i}
\end{aligned}
\tag{40}
$$

where $\sum_{h=k_{i,\bar{t}}} b_i^{k_d-1-h}|\phi_i(x(h), u(h))|$ represents the sum of $b_i^{k_d-1-k_{i,\bar{t}}}|\phi_i(x(k_{i,\bar{t}}), u(k_{i,\bar{t}}))|$ for all $k_{i,\bar{t}} \in [k_0, k_d - 1]/\{k_{i,t}\}$. Combining with (39), we obtain

$$e_i(k_d) > \frac{\left(b_i^{T_i} - b_i^{k_d-k_0}\right)\mu_i}{1 - b_i} - \frac{\left(1 - b_i^{k_d-k_0}\right)\xi^*}{1 - b_i}. \tag{41}$$

Then, $e_i(k_d) > [\varepsilon^*/(1 - b_i)]$ holds as long as

$$K_d = k_d - k_0 \geq \log_{b_i}\frac{b_i^{T_i}\mu_i - \varepsilon^* - \xi^*}{\mu_i - \xi^*} \tag{42}$$

where $\mu_i - \xi^* > 0$ and $b_i^{T_i}\mu_i - \varepsilon^* - \xi^* > 0$ given $\mu_i > \xi^* + \varepsilon^*$ and $T_i < \log_{b_i}[(\xi^* + \varepsilon^*)/\mu_i]$. Note that

$$
\begin{aligned}
\log_{b_i}\frac{b_i^{T_i}\mu_i - \varepsilon^* - \xi^*}{\mu_i - \xi^*} &= \log_{b_i}\left(b_i^{T_i} - \frac{\varepsilon^* + \left(1 - b_i^{T_i}\right)\xi^*}{\mu_i - \xi^*}\right) \\
&> T_i
\end{aligned}
\tag{43}
$$

which implies that (42) ensures $K_d > T_i$. Thus, under condition (36), we can conclude that $e_i(k_d) > \bar{e}_i(k_d) = ([(1 - b_i^{k_d})\varepsilon^*]/[1 - b_i])$ holds, that is, the fault can be detected in a finite time k_d. Finally, since $K_d \in \mathbb{Z}_+$ and according to (42), the upper bound of the FD time can be obtained as (37). ■

Remark 10: The upper bound $\bar{K}_d$ in (37) represents the worst-case detection time, meaning that at most in $\bar{K}_d$ amount of time steps after the fault occurrence at k_0, the fault will definitely be detected under condition (36), and such an upper bound can be estimated using (37). For better understanding, (36) essentially specifies an upper limit for a total number of time instants $k_{i,t}$ (i.e., $T_i < \log_{b_i}[(\xi^* + \varepsilon^*)/\mu_i]$), which are not necessarily consecutive but should be within $[k_0, k_d - 1]$, allowing the magnitude of the associated fault function to be smaller than some bound by μ_i ($\mu_i > \xi^* + \varepsilon^*$). This could be more intuitively understood as: it requires that except at those time instants $k_{i,t}$'s (with the total number T_i), the magnitude of the occurred fault should keep larger than μ_i, so as to enable the estimation of the upper bound of the detection time. In particular, if the occurred fault is sufficiently large (μ_i is large and/or T_i is small), the upper bound of detection time could be guaranteed to be small, indicating that FD under the proposed scheme could be achieved in a rapid manner.

Remark 11: Condition (36) is relatively more restrictive compared to the detectability condition (34) in Theorem 2. However, it should be emphasized that (36) is established only for facilitating the estimation of FD time, which might not be achieved under condition (34). In other words, if only fault detectability is concerned, (34) is sufficient.

V. Simulation Studies

A. Three-Tank System Example

Consider the well-known three-tank system [16] in Fig. 2. Its discrete-time dynamic model can be obtained by employing the Euler discretization with a sampling period $T_s = 0.1$ s

$$\begin{cases} x_1(k+1) = x_1(k) + \frac{T_s}{A}(-q_{13}(k) + u_1(k)) \\ x_2(k+1) = x_2(k) + \frac{T_s}{A}(q_{32}(k) - q_{20}(k) + u_2(k)) \\ x_3(k+1) = x_3(k) + \frac{T_s}{A}(q_{13}(k) - q_{32}(k)) \end{cases} \tag{44}$$

where x_i ($0 < x_i < 0.69$ m, $i = 1, 2, 3$) are the liquid levels in the three tanks; $A = 0.00154$ m^2 is the cross section of three tanks; $q_{13}(k) = r_1 S_p \mathrm{sign}(x_1(k) - x_3(k))\sqrt{2g|x_1(k) - x_3(k)|}$ is the fluid flow rate (m^3/s) between tank 1 and tank 3; $q_{32}(k) = r_3 S_p \mathrm{sign}(x_3(k) - x_2(k))\sqrt{2g|x_3(k) - x_2(k)|}$ is the fluid flow rate (m^3/s) between tank 3 and tank 2; $q_{20} = r_2 S_p \sqrt{2gx_2(k)}$ is the fluid flow of outlet rate (m^3/s) from the tank 2; $S_p = 5 \times 10^{-5}$ m^2 is the cross section of the connection pipes; $g = 9.8$ m/s^2 is the gravity acceleration; and $r_1 = 1$, $r_2 = 0.8$, $r_3 = 1$ are the outflow coefficients. $u_i(k) = \delta(v_i(k))$ ($i = 1, 2$) are the fluid flow of inlet rate (m^3/s) from two pumps, where $\delta(v_i(k)) = 0$ if $v_i < 0$ or $v_i > 1.2 \times 10^{-4}$ m^3/s, and $\delta(v_i(k)) = v_i(k)$ if $0 \le v_i \le 1.2 \times 10^{-4}$ m^3/s; and $v_1(k) = -5S_p(x_1(k) - 0.5) + 0.8S_p(1.5 + \sin(w_1 k))$ and $v_2(k) = -5S_p(x_2(k) - 0.5) + 0.8S_p(1.5 + \cos(w_2 k))$, $w_1 = 0.3$, $w_2 = 0.3$.

In this example, the system dynamics in (44) is assumed to be unknown, that is, $v_1(x(k), u(k)) := x_1(k) + (T_s/A)(-q_{13}(k) + u_1(k))$, $v_2(x(k), u(k)) := x_2(k) + (T_s/A)(q_{32}(k) - q_{20}(k) + u_2(k))$, and $v_3(x(k), u(k)) := x_3(k) + (T_s/A)(q_{13}(k) - q_{32}(k))$. We consider the following four types of small faults.

1) *Faulty Mode 1:* A multiplicative actuator fault occurs in pump 1 by letting $u_1'(k) = u_1(k) + (\alpha_1 - 1)u_1(k)$, where u_1 is the supply flow rate in the nonfault case, and α_1 is the parameter characterizing the magnitude of the fault. In this case, the fault function is $\phi_1^1(x(k), u(k)) := (T_s/A)(\alpha_1 - 1)u_1(k)$. We set $\alpha_1 = 0.8$ for simulation purpose.
2) *Faulty Mode 2:* A multiplicative actuator fault occurs in pump 2 by letting $u_2'(k) = u_2(k) + (\alpha_2 - 1)u_2(k)$. Analogous to faulty mode 1, we denote the fault function as $\phi_2^2(x(k), u(k)) := (T_s/A)(\alpha_2 - 1)u_2(k)$ and set $\alpha_2 = 0.9$.
3) *Faulty Mode 3:* Leakage occurs in tank 1. Assuming the leak is circular in shape and of cross section $S_{l1} = 1 \times 10^{-6}$ m^2, the outflow rate of the leak in tank 1 is obtained as $q_{1f}(k) = r_1 S_{l1}\sqrt{2gx_1(k)}$. The fault function is described by $\phi_1^3(x(k), u(k)) := -(T_s/A)r_1 S_{l1}\sqrt{2gx_1(k)}$.
4) *Faulty Mode 4:* Leakage occurs in tank 2. Similar to faulty mode 3, we assume $q_{2f}(k) = r_2 S_{l2}\sqrt{2gx_2(k)}$ with $S_{l2} = 2 \times 10^{-6}$ m^2 and denote the fault function as $\phi_2^4(x(k), u(k)) := -(T_s/A)r_2 S_{l2}\sqrt{2gx_2(k)}$.

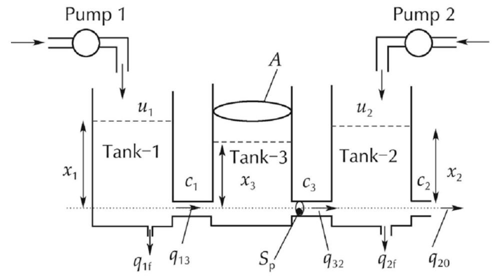

Fig. 2. Three-tank system (Example 1).

Based on the above system setup, we first achieve the accurate identification of the system's uncertain dynamics $v_i(x, u)$ ($i = 1, 2, 3$) under normal mode. To this end, consider the normal system (44), the proposed identifier consisting of (7) and (8) is implemented. The desired learning accuracy is specified by setting $\varepsilon^* = 0.056$, which can be achieved by constructing a sufficiently large number of neurons. Specifically, we construct the RBF networks $\hat{W}_i^T S(x, u)$ in a regular lattice, with nodes $N_n = 29 \times 15 \times 13$, the centers evenly spaced on $[0.510, 0.580] \times [0.430, 0.465] \times [0.475, 0.505]$ and the widths $\eta_t = 0.0025$ ($t = 1, 2, \ldots, 5655$). The design parameters of (7) and (8) are $a_i = 0.1$ and $c_i = 0.04$, respectively. The initial conditions are set as $\hat{W}_i(0) = 0$, $x(0) = [0.54, 0.45, 0.50]^T$, and $\hat{x}(0) = [0, 0, 0]^T$. All the above system setups are kept the same for all $i = 1, 2, 3$. Due to the space limitation, here we only show the simulation plots for identification of the uncertain dynamics $v_1(x, u)$. The system trajectory φ^0 under normal mode is plotted in Fig. 3(a), implying a recurrent φ^0. Fig. 3(b) shows that accurate approximation of the uncertain dynamics $v_1(x, u)$ along the trajectory φ^0 is achieved by $\hat{W}_1^T S(x, u)$. Fig. 3(c) shows the convergence of the weights $\hat{W}_1$, based on which the constant weights $\bar{W}_1$ can be further obtained by $\bar{W}_1 = (1/100)\sum_{k=3901}^{4000} \hat{W}_1(k)$. Using the resulting constant network $\bar{W}_1^T S(x, u)$, accurate approximation of $v_1(x, u)$ in normal mode is also achieved in Fig. 3(d).

Then, we proceed to examine the performance of the proposed sFD scheme. We first compare each faulty dynamics [i.e., $\phi_i(x, u)$] with the associated system uncertain dynamics [i.e., $v_i(x, u)$] in Fig. 4. It is seen that when either one of

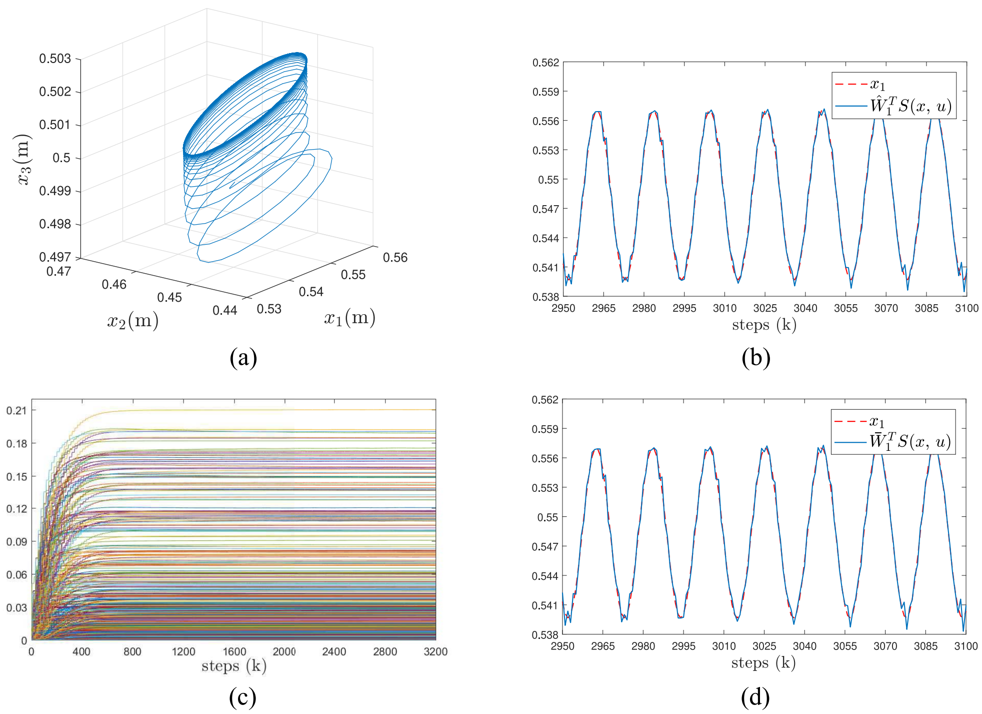

Fig. 3. Identification of the system uncertainty $v_1(x, u)$ in normal mode (Example 1). (a) Normal system trajectory φ^0. (b) Function approximation: $v_1(x, u)$ and $\hat{W}_1^T S(x, u)$. (c) Weight convergence of $\hat{W}_1$. (d) Function approximation: $v_1(x, u)$ and $\bar{W}_1^T S(x, u)$.

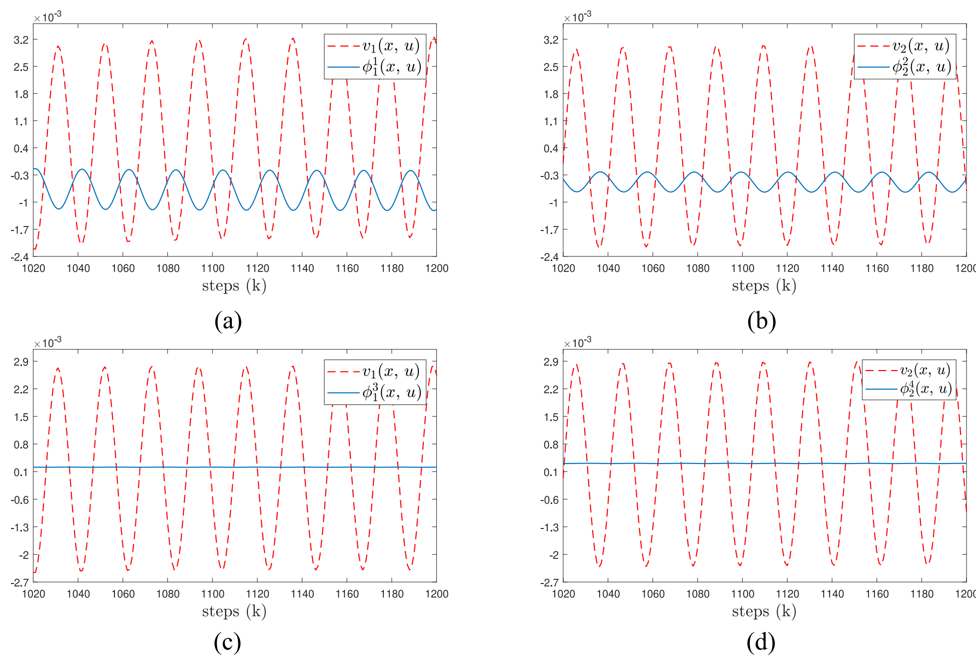

Fig. 4. Time profiles of fault functions and system uncertainty in faulty modes (Example 1). (a) System uncertainty $v_1(x, u)$ and fault function $\phi_1^1(x, u)$ in faulty mode 1. (b) System uncertainty $v_2(x, u)$ and fault function $\phi_2^2(x, u)$ in faulty mode 2. (c) System uncertainty $v_1(x, u)$ and fault function $\phi_1^3(x, u)$ in faulty mode 3. (d) System uncertainty $v_2(x, u)$ and fault function $\phi_2^4(x, u)$ in faulty mode 4.

the faults 1, 2, 3, or 4 occurs, the magnitude of the occurred fault function is much smaller than that of the system uncertainty, meaning that the occurred fault may be hidden within the system uncertainty and is difficult to detect using the existing FD schemes (e.g., [17] and [23]). For simulation purpose, we assume that the occurrence time for each of these small faults is at $k_0 = 1000$. The residual system (29) is implemented by setting $b_1 = b_2 = b_3 = 0.95$. Associated with fault 1, the residual signal e_1 and the adaptive threshold $\bar{e}_1$ are plotted in Fig. 5(a), which shows that $e_1(k)$ becomes larger than $\bar{e}_1(k)$ at $k = k_d = 1014$. Thus, fault 1 can be promptly detected at $k_d = 1014$, 14 time steps after the fault occurrence. The corresponding results for the other two faults are plotted in Fig. 5(b)–(d), respectively.

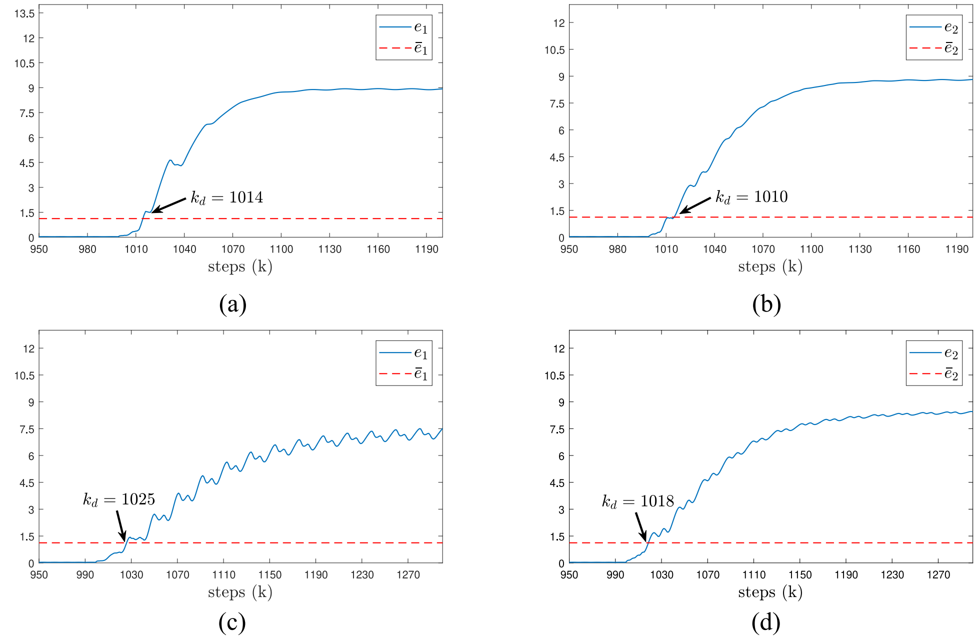

Fig. 5. FD results using the proposed sFD scheme (Example 1). Detection of (a) fault 1, (b) fault 2, (c) fault 3, and (d) fault 4.

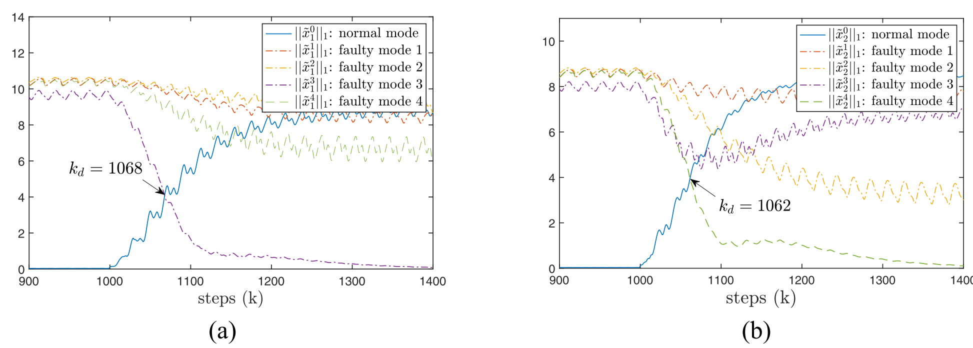

Fig. 6. FD using method of [12] based on SRP (Example 1). Detection of (a) fault 3 and (b) fault 4.

To demonstrate the advantages of our scheme, we compare our results with those of [12] using SRP. Specifically, with the method of [12], we need to first adopt the locally accurate identification method proposed in this article to achieve accurate identification for the uncertain dynamics under all five operation modes (we use $l = 0, 1, 2, 3, 4$ to represent the normal mode, faulty modes 1, 2, 3 and 4, respectively), and obtain the associated constant RBF networks $\bar{W}_i^{lT} S(x, u)$ for all $i = 1, 2, 3$ and $l = 0, 1, 2, 3, 4$. Then, based on the identification results, according to the sFD scheme of [12] using SRP, the following estimators are implemented:

$$\hat{x}_i^l(k) = b_i\Big(\hat{x}_i^l(k-1) - x_i(k-1)\Big) + \bar{W}_i^{lT} S(x(k-1),\ u(k-1)) \tag{45}$$

where $b_i = 0.95$ for all $i = 1, 2, 3$. The resulting residual signals can be processed via an average L_1-norm for sFD decision making, that is, $\|\tilde{x}_i^l(k)\|_1 = (1/K)\sum_{h=k-K}^{k-1} |\hat{x}_i^l(h) - x_i(h)|$ with $K = 20$. The simulation results for cases of faults 3 and 4 are depicted in Fig. 6. It shows that the detection time of faults 3 and 4 are $k_d = 1068$ and $k_d = 1062$, respectively, which are slower than those obtained with our proposed method [as shown in Fig. 5(c) and (d)]. Moreover, it should be pointed out that the SRP-based method needs to construct 15 estimators [in the form of (45)], entailing accurate identification of the system dynamics under the normal and all possible faulty modes. This requires to precisely know all possible types of faults that the system will encounter in *a priori*. While our method based on the adaptive threshold mechanism only needs to implement three estimators [in the form of (29)], entailing accurate identification of the system dynamics under only the normal mode.

B. Duffing Oscillator Example

Consider the Duffing oscillator system [32], its Euler approximation with a sampling period $T_s = 0.1$ s is obtained as

$$\begin{aligned}
x_1(k+1) &= x_1(k) + T_s x_2(k)\\
x_2(k+1)&\\
&= x_2(k) + T_s\Big(-p_2 x_1(k) - p_3 x_1^3(k) - p_1 x_2(k) + q\cos(wT_s k)\Big)\\
&\quad + \beta(k-k_0)\phi_2^s(x(k),\ u(k))
\end{aligned} \tag{46}$$

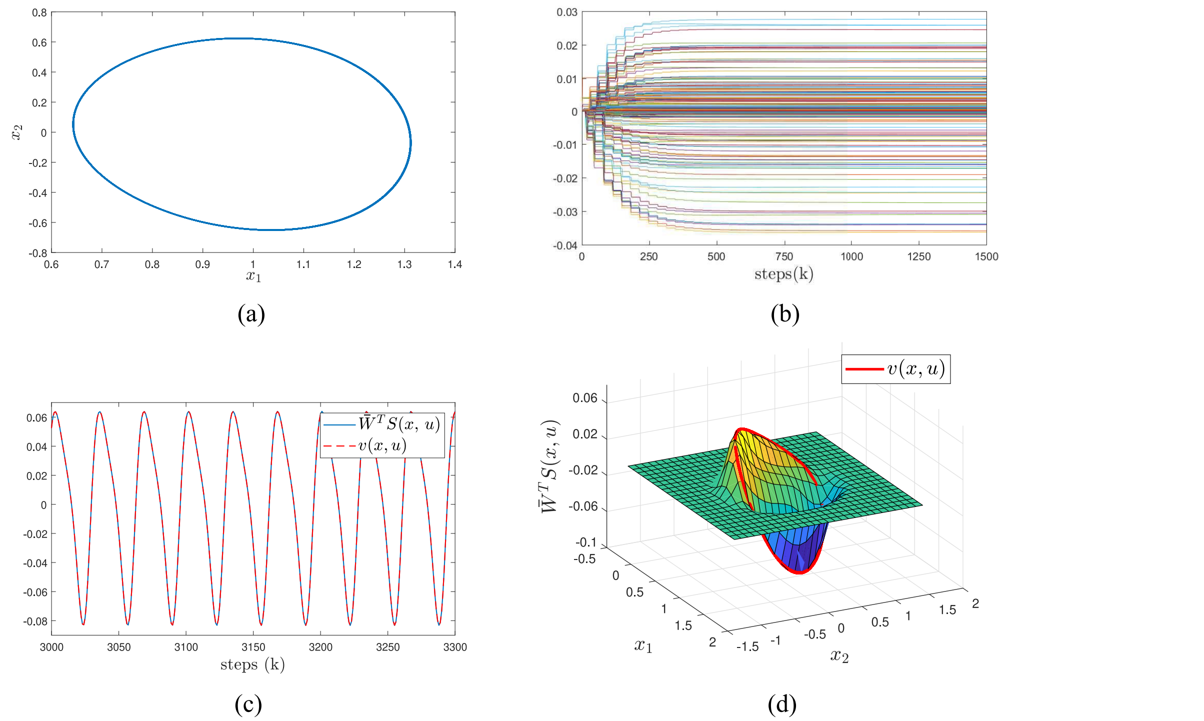

Fig. 7. Identification of the system uncertainty $v(x, u)$ in normal mode (Example 2). (a) Normal system trajectory φ^0. (b) Weight convergence of $\hat{W}$. (c) Function approximation: $v(x, u)$ and $\bar{W}^T S(x, u)$. (d) Approximation in space: $v(x, u)$ and $\bar{W}^T S(x, u)$.

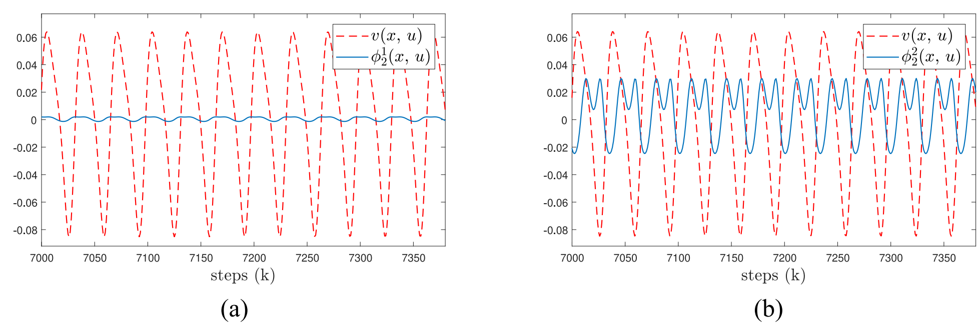

Fig. 8. Time profiles of fault functions and system uncertainty in faulty modes (Example 2). (a) System uncertainty $v(x, u)$ and fault function $\phi_2^1(x, u)$ in faulty mode 1. (b) System uncertainty $v(x, u)$ and fault function $\phi_2^2(x, u)$ in faulty mode 2.

where x_1 and x_2 are the system states; $p_1 = 0.55$, $p_2 = -1.1$, $p_3 = 1$, $w = 1.9$, and $q = 0.62$ are the system parameters; $k_0 = 6500$ is the fault occurrence time; $\phi_2^s(x, u)$ ($s = 1, 2$) represents the fault functions with $\phi_2^1(x(k), u(k)) := \theta_1 T_s \cos(2x_2(k) + x_1(k))$ ($\theta_1 = 0.02$) denoting fault 1, and $\phi_2^2(x(k), u(k)) := \theta_2 T_s \sin(3x_2(k) + x_1(k))$ ($\theta_2 = 0.03$) denoting fault 2. In this example, we assume that $f_1(x(k), u(k)) := x_1(k) + T_s x_2(k)$, $f_2(x(k), u(k)) := x_2(k) + T_s q \cos(wT_s k)$ are the known nominal dynamics of the system, and $v(x(k), u(k)) := -T_s p_2 x_1(k) - T_s p_3 x_1^3(k) - T_s p_1 x_2(k)$ is the system uncertainty.

In the identification phase, consider the normal mode of system (46), we employ the proposed identifier (7), (8) to accurately identify the system uncertainty $v(x, u)$. Setting the desired level of learning accuracy as $\varepsilon^* = 5.48 \times 10^{-4}$, we construct the RBF networks $\hat{W}^T S(x, u)$ in a regular lattice, with nodes $N_n = 23 \times 29$, the centers evenly spaced on $[-0.2, 2] \times [-1.4, 1.4]$ and the widths $\eta_t = 0.1$ ($t = 1, 2, \ldots, 667$). The design parameters are $a_i = 0.1$ and $c_i = 0.1$. The initial conditions are set as $\hat{W}(0) = 0$ and $x(0) = [0.2, 0.4]^T$. Fig. 7(a) shows that the normal system trajectory φ^0 is recurrent. Fig. 7(b) shows the convergence of the weights $\hat{W}$, based on which $\bar{W}$ can be further obtained by $\bar{W} = (1/100) \sum_{k=1401}^{1500} \hat{W}(k)$. Fig. 7(c) and (d) demonstrates the accurate identification of $v(x, u)$ using $\bar{W}^T S(x, u)$.

In the following text, we compare the performance of our sFD scheme with different methods. Specifically, the residual system under our sFD scheme is constructed in the form of (29) with $b_2 = 0.98$, and the adaptive threshold $\bar{e}_2$ is implemented according to (33). We first consider the sFD methods [17], [23] that are also based on the adaptive threshold mechanism but using direct measurement of system dynamics

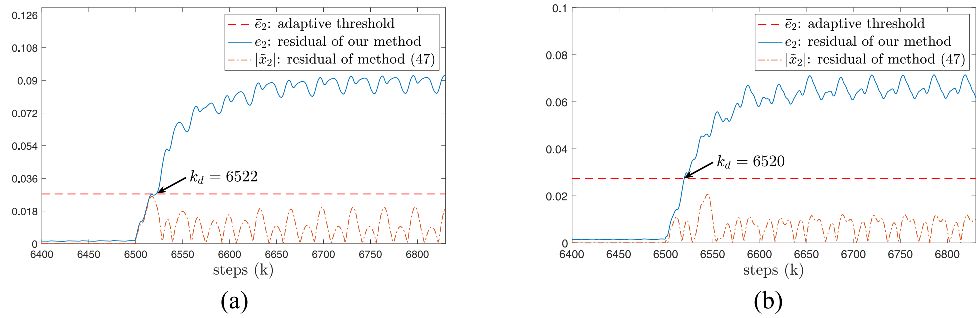

Fig. 9. FD using different methods (Example 2). Detection of (a) fault 1 and (b) fault 2.

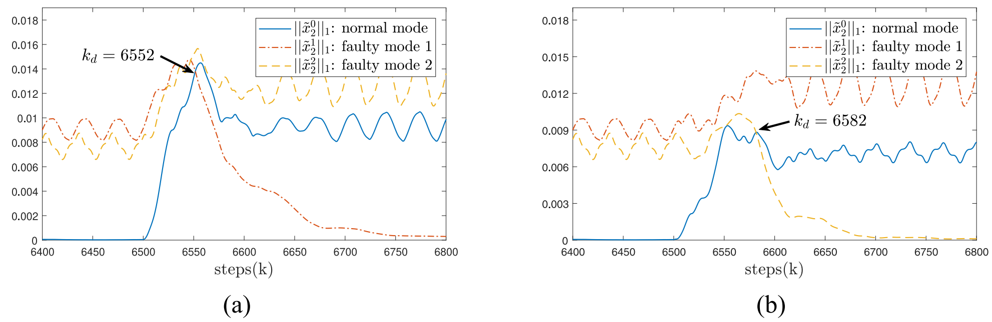

Fig. 10. FD using the method of [12] based on SRP (Example 2). Detection of (a) fault 1 and (b) fault 2.

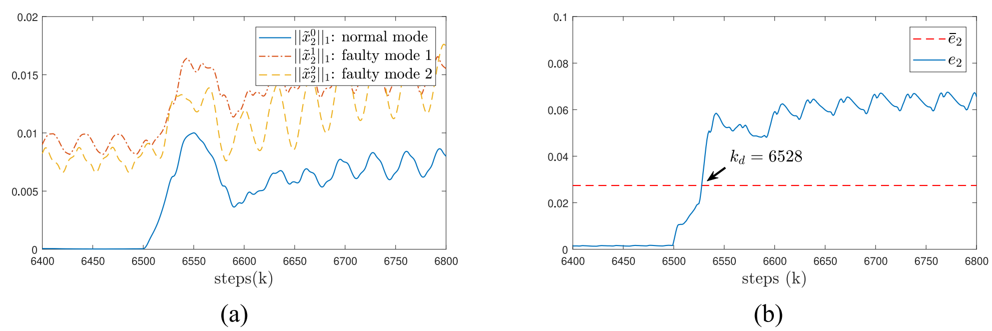

Fig. 11. Detection of fault 3 with different methods (Example 2). (a) SRP-based method of [12]. (b) Our proposed method based on adaptive threshold mechanism.

difference. The associated FD system is constructed as

$$\hat{x}_2(k) = b_2\big(\hat{x}_2(k-1) - x_2(k-1)\big) + x_2(k-1) + T_s \times q\cos(wT_s(k-1)) + \bar{W}^T S(x(k-1), u(k-1)) \tag{47}$$

where $\bar{W}^T S(x, u)$ is the same constant RBF network obtained from the identification phase, $b_2 = 0.98$. The resulting residual signal can be obtained as $|\tilde{x}_2| = |\hat{x}_2 - x_2|$.

Using the above two methods, we carry out the simulations. The time-domain behaviors of the fault functions $\phi_2^1(x, u)$ and $\phi_2^2(x, u)$ as well as the system uncertainty $v(x, u)$ are first plotted in Fig. 8 to show the smallness of faults 1 and 2 compared to the system uncertainty. When fault 1 occurs in system (46), the sFD performance is plotted in Fig. 9(a). It shows that under our scheme, fault 1 is detected at time $k_d = 6522$, whereas no fault is detected under the method (47). This is because the fault 1 function $\phi_2^1(x, u)$ has frequently changing signs [see Fig. 8(a)]. In this case, the difference between the normal system dynamics and faulty system dynamics would be offset, making the residual signal $|\tilde{x}_2|$ stay close to zero. Our method is capable of overcoming this issue due to the use of absolute measurements of the system dynamics difference. Similar comparison results are also observed when fault 2 occurs [see Figs. 9(b) and 8(b)]. These comparisons justify our discussions in Remark 6.

With the same system setup, another comparison study is conducted by using the SRP-based sFD method of [12]. Specific implementation of the SRP-based method follows the same procedure as detailed in (45). The associated estimator parameters are set as $K = 50$ and $b_i = 0.98$ $(i = 1, 2)$. The simulation results are plotted in Fig. 10. It shows that fault 1 is detected at $k_d = 6552$ [Fig. 10(a)] and fault 2 at $k_d = 6582$ [Fig. 10(b)], which are slightly slower than the detection results obtained with our proposed method (Fig. 9). Another important advantage of our method lies in its capability of detecting unknown faults. Specifically, we consider a new coming fault that is not known in *a priori*, denoted as fault 3 with the associated fault function $\phi_2^3(x(k), u(k)) := -0.0196\sin(x_1(k))^2$. Since fault 3 is not *a priori* known, we adopt the same estimators as above under the SRP-based method of [12], and compare its FD performance with that of our method. The simulation results are plotted in Fig. 11. Fig. 11(a) shows the FD performance with the method of [12], where the residual signal $\|\tilde{x}_2^0\|_1$ (associated with the normal mode) remains the smallest one even when fault 3 occurs, indicating its incapability of detecting fault 3. In contrast, our method is still capable of promptly detecting fault 3 at $k_d = 6527$ [see Fig. 11(b)].

VI. Conclusion

In this article, a novel adaptive dynamics learning-based scheme has been proposed for sFD of discrete-time nonlinear uncertain systems. First, to overcome the challenge that small faults may be hidden within the system uncertainty, a novel adaptive dynamics learning approach was developed to achieve locally accurate approximation of the unknown system dynamics in the normal mode, where the learned knowledge can be obtained, represented, and stored in constant RBF NNs. Based on this, a residual system was developed by using the absolute measurements of the difference between the monitored system dynamics and the normal system dynamics. An adaptive threshold was then designed for real-time sFD decision making. Finally, the effectiveness and advantages of the proposed approach have been demonstrated through both rigorous analysis and extensive numerical simulations. For future work, it is promising to extend this new sFD methodology to more challenging problems, for example, small fault isolation.

References

[1] S. Yin, H. Gao, J. Qiu, and O. Kaynak, "Fault detection for nonlinear process with deterministic disturbances: A just-in-time learning based data driven method," *IEEE Trans. Cybern.*, vol. 47, no. 11, pp. 3649–3657, Nov. 2017.

[2] H. Chen and S. Lu, "Fault diagnosis digital method for power transistors in power converters of switched reluctance motors," *IEEE Trans. Ind. Electron.*, vol. 60, no. 2, pp. 749–763, Feb. 2013.

[3] J. Seshadrinath, B. Singh, and B. K. Panigrahi, "Vibration analysis based interturn fault diagnosis in induction machines," *IEEE Trans. Ind. Informat.*, vol. 10, no. 1, pp. 340–350, Feb. 2014.

[4] X.-J. Li and G.-H. Yang, "Fault detection in finite frequency domain for Takagi–Sugeno fuzzy systems with sensor faults," *IEEE Trans. Cybern.*, vol. 44, no. 8, pp. 1446–1458, Aug. 2014.

[5] Q. Zhao and Z. Xu, "Design of a novel knowledge-based fault detection and isolation scheme," *IEEE Trans. Syst., Man, Cybern. B, Cybern.*, vol. 34, no. 2, pp. 1089–1095, Apr. 2004.

[6] Z. Gao, C. Cecati, and S. X. Ding, "A survey of fault diagnosis and fault-tolerant techniques—Part I: Fault diagnosis with model-based and signal-based approaches," *IEEE Trans. Ind. Electron.*, vol. 62, no. 6, pp. 3757–3767, Jun. 2015.

[7] Z. Gao, C. Cecati, and S. X. Ding, "A survey of fault diagnosis and fault-tolerant techniques—Part II: Fault diagnosis with knowledge-based and hybrid/active approaches," *IEEE Trans. Ind. Electron.*, vol. 62, no. 6, pp. 3768–3774, Jun. 2015.

[8] D. Koenig, "Unknown input proportional multiple-integral observer design for linear descriptor systems: Application to state and fault estimation," *IEEE Trans. Autom. Control*, vol. 50, no. 2, pp. 212–217, Feb. 2005.

[9] X. Su, P. Shi, L. Wu, and Y.-D. Song, "Fault detection filtering for nonlinear switched stochastic systems," *IEEE Trans. Autom. Control*, vol. 61, no. 5, pp. 1310–1315, May 2016.

[10] F. N. Chowdhury and W. Chen, "Fault detection in dynamic systems: A new approach via total measurable fault information," in *Proc. IEEE Int. Conf. Control Appl. (CCA)*, 2007, pp. 946–951.

[11] Y. Wu, B. Jiang, N. Lu, and D. Zhou, "ToMFIR-based incipient fault detection and estimation for high-speed rail vehicle suspension system," *J. Frankl. Inst.*, vol. 352, no. 4, pp. 1672–1692, 2015.

[12] C. Wang and T. Chen, "Rapid detection of small oscillation faults via deterministic learning," *IEEE Trans. Neural Netw.*, vol. 22, no. 8, pp. 1284–1296, Aug. 2011.

[13] T. Chen, C. Wang, G. Chen, Z. Dong, and D. J. Hill, "Small fault detection for a class of closed-loop systems via deterministic learning," *IEEE Trans. Cybern.*, vol. 49, no. 3, pp. 897–906, Mar. 2019.

[14] T. Hall, S. Beecham, D. Bowes, D. Gray, and S. Counsell, "A systematic literature review on fault prediction performance in software engineering," *IEEE Trans. Softw. Eng.*, vol. 38, no. 6, pp. 1276–1304, Nov./Dec. 2012.

[15] S. Simani, C. Fantuzzi, and R. J. Patton, *Model-Based Fault Diagnosis in Dynamic Systems Using Identification Techniques*. New York, NY, USA: Springer, 2013.

[16] X. Zhang, M. M. Polycarpou, and T. Parisini, "A robust detection and isolation scheme for abrupt and incipient faults in nonlinear systems," *IEEE Trans. Autom. Control*, vol. 47, no. 4, pp. 576–593, Apr. 2002.

[17] R. M. Ferrari, T. Parisini, and M. M. Polycarpou, "A robust fault detection and isolation scheme for a class of uncertain input–output discrete-time nonlinear systems," in *Proc. IEEE Amer. Control Conf.*, 2008, pp. 2804–2809.

[18] C. Keliris, M. M. Polycarpou, and T. Parisini, "A robust nonlinear observer-based approach for distributed fault detection of input–output interconnected systems," *Automatica*, vol. 53, pp. 408–415, Mar. 2015.

[19] C. Wang and D. J. Hill, *Deterministic Learning Theory for Identification, Recognition, and Control*. Boca Raton, FL, USA: CRC, 2009.

[20] T. Liu, C. Wang, and D. J. Hill, "Learning from neural control of nonlinear systems in normal form," *Syst. Control Lett.*, vol. 58, no. 9, pp. 633–638, 2009.

[21] C. Yuan, S. Licht, and H. He, "Formation learning control of multiple autonomous underwater vehicles with heterogeneous nonlinear uncertain dynamics," *IEEE Trans. Cybern.*, vol. 48, no. 10, pp. 2920–2934, Oct. 2018.

[22] T. Chen, C. Wang, and D. J. Hill, "Small oscillation fault detection for a class of nonlinear systems with output measurements using deterministic learning," *Syst. Control Lett.*, vol. 79, pp. 39–46, May 2015.

[23] R. M. G. Ferrari, T. Parisini, and M. M. Polycarpou, "Distributed fault detection and isolation of large-scale discrete-time nonlinear systems: An adaptive approximation approach," *IEEE Trans. Autom. Control*, vol. 57, no. 2, pp. 275–290, Feb. 2012.

[24] J. Sarangapani, *Neural Network Control of Nonlinear Discrete-Time Systems*. Boca Raton, FL, USA: CRC, 2006.

[25] C. Yuan and C. Wang, "Persistency of excitation and performance of deterministic learning," *Syst. Control Lett.*, vol. 60, no. 12, pp. 952–959, 2011.

[26] W. Chen, S. Hua, and S. S. Ge, "Consensus-based distributed cooperative learning control for a group of discrete-time nonlinear multi-agent systems using neural networks," *Automatica*, vol. 50, no. 9, pp. 2254–2268, 2014.

[27] J. Park and I. W. Sandberg, "Universal approximation using radial-basis-function networks," *Neural Comput.*, vol. 3, no. 2, pp. 246–257, Jun. 1991.

[28] M. Poewell, *The Theory of Radial Basis Function Approximation*. Oxford, U.K.: Clarendon Press, 1992.

[29] C. Wang and D. J. Hill, "Learning from neural control," *IEEE Trans. Neural Netw.*, vol. 17, no. 1, pp. 130–146, Jan. 2006.

[30] C. Yuan and C. Wang, "Design and performance analysis of deterministic learning of sampled-data nonlinear systems," *Sci. China Inf. Sci.*, vol. 57, no. 3, pp. 1–18, 2014.

[31] F. Yang and C. Wang, "Pattern-based NN control of a class of uncertain nonlinear systems," *IEEE Trans. Neural Netw. Learn. Syst.*, vol. 29, no. 4, pp. 1108–1119, Apr. 2018.

[32] I. Kovacic and M. J. Brennan, *The Duffing Equation: Nonlinear Oscillators and Their Behaviour*. Hoboken, NJ, USA: Wiley, 2011.

[33] F. J. Narcowich, N. Sivakumar, and J. D. Ward, "On condition numbers associated with radial-function interpolation," *J. Math. Anal. Appl.*, vol. 186, no. 2, pp. 457–485, 1994.

[34] W. Wu, C. Wang, and C. Yuan, "Deterministic learning from sampling data," *Neurocomputing*, vol. 358, no. 17, pp. 456–466, 2019.

[35] T. Zheng and C. Wang, "Relationship between persistent excitation levels and RBF network structures, with application to performance analysis of deterministic learning," *IEEE Trans. Cybern.*, vol. 47, no. 10, pp. 3380–3392, Oct. 2017.

[36] H. Zhang, J. Han, C. Luo, and Y. Wang, "Fault-tolerant control of a nonlinear system based on generalized fuzzy hyperbolic model and adaptive disturbance observer," *IEEE Trans. Syst., Man, Cybern., Syst.*, vol. 47, no. 8, pp. 2289–2300, Aug. 2017.

[37] M. Van, S. S. Ge, and H. Ren, "Finite time fault tolerant control for robot manipulators using time delay estimation and continuous nonsingular fast terminal sliding mode control," *IEEE Trans. Cybern.*, vol. 47, no. 7, pp. 1681–1693, Jul. 2017.

[38] H. Zhang, Y. Cui, and Y. Wang, "Hybrid fuzzy adaptive fault-tolerant control for a class of uncertain nonlinear systems with unmeasured states," *IEEE Trans. Fuzzy Syst.*, vol. 25, no. 5, pp. 1041–1050, Oct. 2017.

[39] H. Li, Z. Chen, L. Wu, H.-K. Lam, and H. Du, "Event-triggered fault detection of nonlinear networked systems," *IEEE Trans. Cybern.*, vol. 47, no. 4, pp. 1041–1052, Apr. 2017.

[40] H. Zhang, J. Han, Y. Wang, and X. Liu, "Sensor fault estimation of switched fuzzy systems with unknown input," *IEEE Trans. Fuzzy Syst.*, vol. 26, no. 3, pp. 1114–1124, Jun. 2018.

[41] R. H. Kwong and D. L. Yonge-Mallo, "Fault diagnosis in discrete-event systems with incomplete models: Learnability and diagnosability," *IEEE Trans. Cybern.*, vol. 45, no. 7, pp. 1236–1249, Jul. 2015.

[42] J. Zhang, C. Yuan, P. Stegagno, W. Zeng, and C. Wang, "Small fault detection from discrete-time closed-loop control using fault dynamics residuals," *Neurocomputing*, vol. 365, no. 6, pp. 239–248, 2019.

Jingting Zhang received the B.E. degree from the Department of Automation Science and Engineering, South China University of Technology, Guangzhou, China, in 2017. She is currently pursuing the Ph.D. degree with the Department of Mechanical, Industrial and Systems Engineering, University of Rhode Island, Kingston, RI, USA.

Her current research interests include adaptive neural network and nonlinear systems, fault diagnosis, and deterministic learning theory.

Chengzhi Yuan (M'14) received the B.S. and M.S. degrees in control theory and applications from the South China University of Technology, Guangzhou, China, in 2009 and 2012, respectively, and the Ph.D. degree in mechanical engineering from North Carolina State University, Raleigh, NC, USA, in 2016.

He is currently an Assistant Professor with the Mechanical, Industrial and Systems Engineering Department, University of Rhode Island, Kingston, RI, USA. He has authored and coauthored over 80 journal articles and conference papers. His current research interests include dynamic systems and control theory, with particular focuses on analytical adaptive learning and control, hybrid systems, and multirobot distributed control.

Dr. Yuan has served extensively as an associate editor, the chair and co-chair, and the program committee member in numerous international conferences. He served in the Technical Program Committee for the American Control Conference in 2018. He served as a Guest Editor for the special issue in the journal of the *IET Control Theory and Applications* in 2018 and *Advances in Mechanical Engineering* in 2017.

Paolo Stegagno (M'10) received the Ph.D. degree in system engineering from the Sapienza University of Rome, Rome, Italy, in 2012.

In 2010, he was a Visiting Scholar with the University of Minnesota, Minneapolis, MN, USA. From 2012 to 2013, he was a Postdoctoral Fellow with the Sapienza University of Rome. From 2013 to 2016, he was a Research Scientist with the Autonomous Robotics and Human–Machine Systems Group, Max Planck Institute for Biological Cybernetics, Tübingen, Germany, where he has also been the Project Leader since 2014. He was a Postdoctoral Fellow with the Ocean Engineering Department, University of Rhode Island, Kingston, RI, USA, for one year, where he joined the Electrical, Computer and Biomedical Engineering Department as an Assistant Professor. His current research interests include mobile robotics, multirobot systems, robotic swarms, and unmanned aerial vehicles, with a focus on sensing, estimation, localization, and interaction with humans.

Dr. Stegagno has been an Associate Editor of the IEEE/RSJ International Conference on Intelligent Robots and Systems since 2014.

Haibo He (SM'11–F'18) received the B.S. and M.S. degrees in electrical engineering from the Huazhong University of Science and Technology, Wuhan, China, in 1999 and 2002, respectively, and the Ph.D. degree in electrical engineering from Ohio University, Athens, OH, USA, in 2006.

From 2006 to 2009, he was an Assistant Professor with the Department of Electrical and Computer Engineering, Stevens Institute of Technology, Hoboken, NJ, USA. He is currently the Robert Haas Endowed Chair Professor with the Department of Electrical, Computer, and Biomedical Engineering, University of Rhode Island, Kingston, RI, USA. He has published one sole-authored research book (Wiley), edited one book (Wiley-IEEE), six conference proceedings (Springer), and authored and coauthored over 300 peer-reviewed journals and conference papers. His current research interests include adaptive learning and control, computational intelligence, machine learning, data mining, and various applications.

Dr. He was a recipient of the IEEE International Conference on Communications Best Paper Award in 2014, the IEEE Computational Intelligence Society (CIS) Outstanding Early Career Award in 2014, and the National Science Foundation CAREER Award in 2011. He was the Chair of IEEE CIS Emergent Technologies Technical Committee in 2015 and the IEEE CIS Neural Networks Technical Committee from 2013 to 2014. He served as the General Chair of 2014 IEEE Symposium Series on Computational Intelligence (IEEE SSCI'14, Orlando, FL, USA). He is currently the Editor-in-Chief of the IEEE TRANSACTIONS ON NEURAL NETWORKS AND LEARNING SYSTEMS.

Cong Wang (M'02) received the B.E. and M.E. degrees from the Beijing University of Aeronautic and Astronautics, Beijing, China, in 1989 and 1997, respectively, and the Ph.D. degree from the Department of Electrical and Computer Engineering, National University of Singapore, Singapore, in 2002.

From 2001 to 2004, he was a Postdoctoral Researcher with the Department of Electronic Engineering, City University of Hong Kong, Hong Kong. His current research interests include intelligent control, neural networks, nonlinear systems and control, dynamical pattern recognition, pattern-based control, dynamical systems, and oscillation fault diagnosis.